AD-A043 692 NAVAL UNDERWATER SYSTEMS CENTER NEWPORT R I F/G 17/3
POSITION AND VELOCITY ESTIMATION VIA BEARING OBSERVATIONS.(U)
JUN 77 A G LINDGREN, K F GONG

UNCLASSIFIED NUSC-TR-5260 NL

1 OF 1
AD A043692

END
DATE FILMED
9-77
DDC

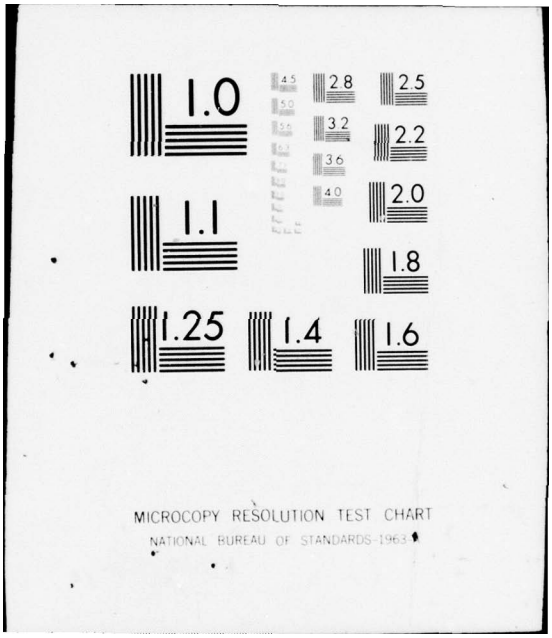
1.0
1.1
1.25
1.4
1.6
1.8
2.0
2.2
2.5
2.8
3.2
3.6
4.0
4.5
5.0
5.6
MICROCOPY RESOLUTION TEST CHART
NATIONAL BUREAU OF STANDARDS-1963-A

NUSC Technical Report 5260

(2)

Position and Velocity Estimation Via Bearing Observations

A. G. Lindgren
K. F. Gong
Combat Control Systems Department

15 June 1977

NAVAL UNDERWATER SYSTEMS CENTER
Newport Laboratory

PREFACE

This investigation was conducted under NUSC Project No. A45103, "Underwater Fire Control Target Localization and Target Motion Analysis," Principal Investigator—J. S. Davis (Code 3522), and under Navy Subproject and Task No. SF-33341422/18406. The sponsoring activity is the Naval Sea Systems Command, Program Manager—W. Welsh (SEA-03424).

The Technical Reviewer for this report was J.S. Davis.

REVIEWED AND APPROVED: 15 June 1977

E. L. Messere
Head, Combat Control Systems Department

The authors of this report are located at the Newport Laboratory, Naval Underwater Systems Center, Newport, Rhode Island 02840.

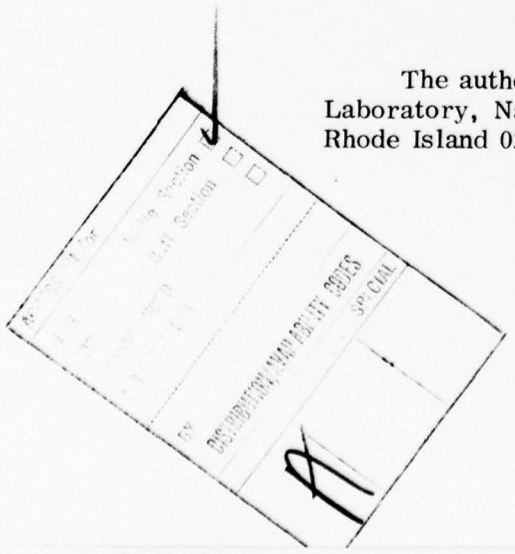

UNCLASSIFIED

SECURITY CLASSIFICATION OF THIS PAGE (When Data Entered)

REPORT DOCUMENTATION PAGE	READ INSTRUCTIONS BEFORE COMPLETING FORM
1 REPORT NUMBER: TR 5260	2 GOVT ACCESSION NO. / 3 RECIPIENT'S CATALOG NUMBER
4 TITLE (and Subtitle): POSITION AND VELOCITY ESTIMATION VIA BEARING OBSERVATIONS.	5 TYPE OF REPORT & PERIOD COVERED: Technical rept. / 6 PERFORMING ORG. REPORT NUMBER
7 AUTHOR(s): A. G. Lindgren, K. F. Gong	8 CONTRACT OR GRANT NUMBER(s): 62633N
9 PERFORMING ORGANIZATION NAME AND ADDRESS: Naval Underwater Systems Center, Newport Laboratory, Newport, Rhode Island 02840	10 PROGRAM ELEMENT, PROJECT, TASK AREA & WORK UNIT NUMBERS: Navy Subproject and Task No. SF-33341422/18406
11 CONTROLLING OFFICE NAME AND ADDRESS: Naval Sea Systems Command (SEA-03424), Washington, D C. 20362	12 REPORT DATE: 15 June 1977 / 13 NUMBER OF PAGES: 62
14 MONITORING AGENCY NAME & ADDRESS (if different from Controlling Office): NUSC-TR-5264 (12) 65 p.	15 SECURITY CLASS. (of this report): UNCLASSIFIED / 15a DECLASSIFICATION/DOWNGRADING SCHEDULE
16 DISTRIBUTION STATEMENT (of this Report): Approved for public release; distribution unlimited.	
17 DISTRIBUTION STATEMENT (of the abstract entered in Block 20, if different from Report): (16) F33341 (17) SF33341422	
18 SUPPLEMENTARY NOTES	
19 KEY WORDS (Continue on reverse side if necessary and identify by block number): Target Motion Analysis; Bearings-Only TMA; TMA Algorithms	

406 068

20 ABSTRACT (Continue on reverse side if necessary and identify by block number)

The theory of estimating the position and motion of a radiating source traveling at a constant velocity from a history of bearing measurements is presented. The dynamic process for the single observer case is found to be unobservable when the observer velocity is constant, and estimation of the complete target state requires an observer maneuver. Discrete changes in the observer velocity result in piecewise convergence of the state estimate. The relationship between recursive least-squares estimation and Kalman filtering is detailed for such →

DD FORM 1 JAN 73 1473 EDITION OF 1 NOV 65 IS OBSOLETE S/N 0102-014-6601

UNCLASSIFIED

SECURITY CLASSIFICATION OF THIS PAGE (When Data Entered)

20. Abstract (Cont'd)

processes, and an algorithm—including initialization—is presented that exhibits consistent behavior for all target observer geometries examined. Experimental studies are presented. Minimum norm solutions are provided during the initial phase of the problem with convergence to a complete solution following observer maneuvers resulting in the process becoming observable. Although emphasis is given to the case of a single moving observer, the estimation algorithm is capable of processing bearing information from multiple platforms.

TABLE OF CONTENTS

LIST OF ILLUSTRATIONS ii

LIST OF TABLES iii

LIST OF SYMBOLS iii

FOREWORD vi

INTRODUCTION 1

MODELING OF THE TARGET-OBSERVER DYNAMICS 3

ESTIMATION OF TARGET STATES 6
Linear Estimation 6
Properties of Linear Estimators and Initialization of the Recursive Algorithm 11
Application to the Motion Analysis Problem 17

IMPLEMENTATION OF THE SINGLE OBSERVER TMA ALGORITHM. . 20

PROPERTIES OF THE TMA SOLUTION. 23

EXPERIMENTAL RESULTS 25

SUMMARY AND CONCLUSIONS 45

REFERENCES 46

APPENDIX A—OBSERVABILITY OF THE NOISE-FREE TARGET-OBSERVER PROCESS A-1

APPENDIX B—MATRIX INVERSION IDENTITIES. B-1

APPENDIX C—RECURSIVE COMPUTATION OF THE MINIMUM NORM SOLUTION C-1

APPENDIX D—SUMMARY OF THE APPLICATION OF THE EXTENDED KALMAN FILTER TO THE MOTION ANALYSIS PROBLEM D-1

LIST OF ILLUSTRATIONS

Figure		Page
1	Geometry for General Two-Dimensional Bearings-Only Motion Analysis Problem.	1
2	Special Case: All Bearing Measurements Generated by a Single Moving Observer	2
3a	Block Diagram of Observer Dynamics, Measurement Equation, and Estimator for Unknown Target State $x_T(k)$	18
3b	Equivalent Block Diagram of Figure 3a	18
3c	Block Diagram of Estimator for $x_R(k)$ Resulting from Simplification of Figure 3b.	18
4	Simulation Diagram of Motion Analysis System	25
5a	Vehicle Tracks for Target-Observer Geometry No. 1	27
5b	Actual and Estimated Relative Motion During the First Leg for Various Initial Range Estimates (Geometry No. 1).	28
5c	Actual and Estimated Target Tracks for Various Initial Range Estimates (Geometry No. 1)	29
5d	Actual and Estimated Relative X-Position (r_x) as a Function of Elapsed Time (Geometry No. 1).	30
5e	Actual and Estimated Relative Y-Position (r_y) as a Function of Elapsed Time (Geometry No. 1).	31
5f	Actual and Estimated Target Velocity Along the X-Axis (Geometry No. 1).	32
5g	Actual and Estimated Target Velocity Along the Y-Axis (Geometry No. 1).	33
6a	Range Error for Various Initialization Parameters (Geometry No. 1).	34
6b	Target Course Error for Various Initialization Parameters (Geometry No. 1).	35
6c	Target Speed Error for Various Initialization Parameters (Geometry No. 1).	36
7a	Vehicle Tracks for Target-Observer Geometry No. 2.	37
7b	Range Error for Geometry No. 2.	38
7c	Target Course Error for Geometry No. 2	39
7d	Target Speed Error for Geometry No. 2	40
8a	Vehicle Tracks for Target-Observer Geometry No. 3.	41
8b	Range Error for Geometry No. 3	42
8c	Target Course Error for Geometry No. 3	43
8d	Target Speed Error for Geometry No. 3	44
A-1	Existence of a One-Parameter Family of Solutions Scaled by $\hat{r}_S(0)$ in the First Leg of the Bearings-Only Motion Analysis Problem	A-3

LIST OF TABLES

Table		Page
1	Summary of the Recursive Estimation of the Relative Target State $x_R(k)$	19
2	Summary of the Normalized Recursive Algorithm	22

LIST OF SYMBOLS

$V_{Tx}(k)$	X-component of target velocity
$V_{Ty}(k)$	Y-component of target velocity
$V_T(k)$	Target velocity vector
$r_{Tx}(k)$	X-component of target position
$r_{Ty}(k)$	Y-component of target position
$r_T(k)$	Target position vector
$x_T(k)$	Target state vector
$V_{Ox}(k)$	X-component of observer velocity
$V_{Oy}(k)$	Y-component of observer velocity
$r_{Ox}(k)$	X-component of observer position
$r_{Oy}(k)$	Y-component of observer position
$x_O(k)$	Observer state vector
$x_R(k)$	Relative target state vector, i.e., $x_R(k) = x_T(k) - x_O(k)$
$r_x(k)$	X-component of relative position, i.e., $r_x(k) = r_{Tx}(k) - r_{Ox}(k)$
$r_y(k)$	Y-component of relative position, i.e., $r_y(k) = r_{Ty}(k) - r_{Oy}(k)$
$V_x(k)$	X-component of relative velocity, i.e., $V_x(k) = V_{Tx}(k) - V_{Ox}(k)$
$V_y(k)$	Y-component of relative velocity, i.e., $V_y(k) = V_{Ty}(k) - V_{Oy}(k)$
$x(k)$	State vector
$\hat{x}_{LS}(k)$	Least-squares estimate of $x(k)$

LIST OF SYMBOLS (Cont'd)

$\hat{x}(0\|0)$	Initial state estimate
$\hat{x}(k\|k)$	Estimate of $x(k)$ conditioned by k measurements
$\hat{x}(k\|k-1)$	Estimate of $x(k)$ conditioned by $k-1$ measurements
$r_s(k)$	Slant range
t_s	Time increment between samples
$\beta(k)$	Noise-free target bearing
$\nu(k)$	Bearing measurement noise (random Gaussian)
$\beta_m(k)$	Measured bearing
$z(k)$	Measurement at time kt_s, i.e., $z(k) = H(k)x_o(k)$
$\eta(k)$	Cross-range noise
$H(k)$	Measurement matrix
$Z(k)$	Vector of available measurements, i.e., column of $[z(k)\ z(k-1)\ldots z(1)]$
$N(k)$	Vector of available measurement noise, i.e., column of $[\eta(k)\ \eta(k-1)\ldots\eta(1)]$
$\sigma_\nu^2(k)$	Variance of bearing measurement noise $\nu(k)$
$M_\eta(k)$	Mean value of cross-range noise $\eta(k)$
$\sigma_\eta^2(k)$	Variance of cross-range noise $\eta(k)$
$R(k)$	Measurement covariance matrix of $N(k)$
$\Phi(k+1,k)$	Discrete state transition matrix
$L(\cdot)$	Cost function
$\|\|(\cdot)\|\|$	Norm of $(\cdot)$
$P_x(k)$	Covariance matrix of $x(k)$
$P(k\|k)$	Estimated error covariance matrix at $t = kt_s$, conditioned by k measurements

LIST OF SYMBOLS (Cont'd)

$P(k\|k-1)$	Estimated error covariance matrix at $t = kt_s$, conditioned by $k-1$ measurements
$P(0\|0)$ or P_0	Initial estimate of the error covariance matrix
$P_N(k)$	Range-normalized error covariance matrix
$K(k)$	System gain matrix
T or T_1	Orthogonal transformation matrix
Λ or Ω	Diagonal matrix
n	Number of states
$>(a,b)<$	Outer product of (a, b)
$E[\cdot]$	Expected value of $[\cdot]$
$[\cdot]'$	Transpose of $[\cdot]$
$[\cdot]^{-1}$	Inverse of $[\cdot]$
$[\cdot]^{\#}$	Pseudoinverse of $[\cdot]$
$Tr[\cdot]$	Trace of $[\cdot]$
$\det[\cdot]$	Determinant of $[\cdot]$
I	Identity matrix
$[0]$	Null matrix
$\phi(k, j)$	Optimal state transition matrix
$A(k)$	Matrix relating state to available measurements

FOREWORD

Target motion analysis (TMA) is a critical function in naval combat control systems. In many situations, bearing is the only information available and bearings-only target motion analysis is the foundation of the TMA process. This report is the result of research directed toward the estimation of target position and motion parameters via bearing measurements generated by a single moving observer. However, the modeling and theory presented are applicable to the general case of multiple moving or stationary observers. The estimation algorithm can also be applied to navigational systems in a situation where a vehicle observes the bearings to transmitters of known location. The theory presented in this report can be extended to include the processing of multiple sensor information when available to improve the performance and capability of TMA in naval applications. Implementation of this estimation algorithm should provide significant improvement in the convergence properties of automatic TMA solutions.

POSITION AND VELOCITY ESTIMATION VIA BEARING OBSERVATIONS

INTRODUCTION

The problem of estimating the position and velocity of a body traveling on a straight-line course from a history of bearing measurements is considered in this report. The body is assumed to emit an appropriate signal; and, in the general two-dimensional problem, the bearings are viewed from observers confined to a plane that includes the target. The situation is illustrated in figure 1 where it is desired to estimate the position vector $r_T = (r_{Tx} r_{Ty})'$ and velocity vector $V_T = (V_{Tx} V_{Ty})'$ of the observed body from noise-corrupted measurements of the bearing β. The inverse situation where the body observes the bearings to transmitters of known location represents a system capable of providing navigational information.

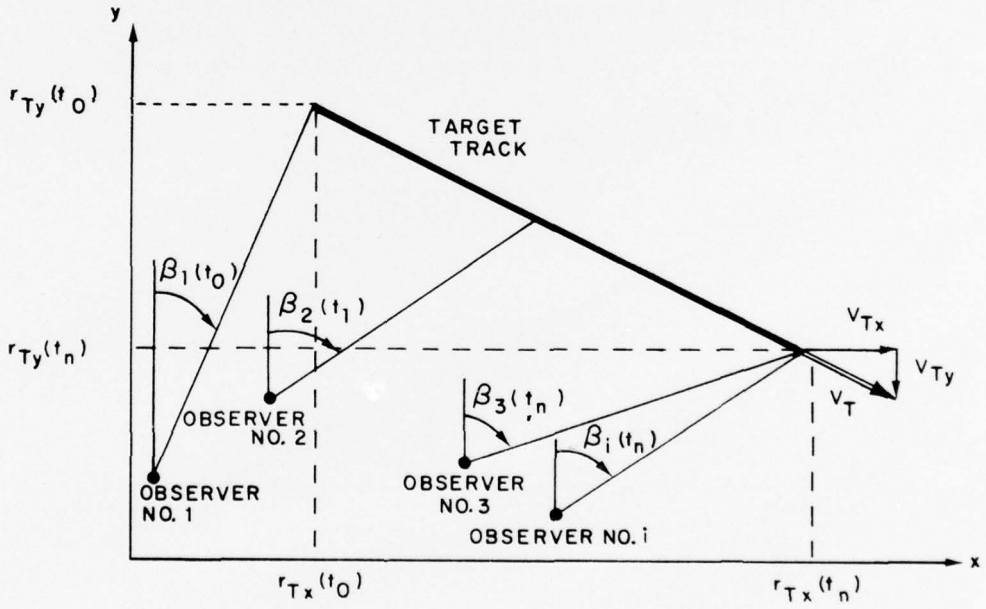

Figure 1. Geometry for General Two-Dimensional Bearings-Only Motion Analysis Problem

Defining $x_T = (r_{Tx} r_{Ty} V_{Tx} V_{Ty})'$ as the target state, $x_O = (r_{Ox} r_{Oy} V_{Ox} V_{Oy})'$ as the observer state, and $x_R = x_T - x_O$ as the relative target state, the problem of determining x_R has been posed as a nonlinear estimation problem. A common method employed to obtain a solution has been the extended

Kalman filter, although this method has experienced convergence difficulties.[1,2] The formulation of the motion analysis problem as presented in this report is exact and automatically casts the model in a linear form with Gaussian measurement perturbations. Thus, linear estimation techniques apply, and the problem of algorithm stability normally encountered in nonlinear estimation is avoided and improved system performance is achieved.

The modeling and theory presented provide a solution to the general motion analysis problem. However, this report is devoted almost exclusively to the important special case where all bearing measurements are generated by a single moving observer as illustrated in figure 2. The dynamic model that results when the observer is also traveling at a constant velocity represents an unobservable process.[1,2] In a typical situation, observer motion is often restricted to straight-line segments and each segment is termed a "leg" or "phase" of the motion analysis problem. It is well known that only a relative solution (i.e., estimates normalized by the slant range r_S) can be obtained on the first leg. To obtain an observable process for the purpose of estimating the actual value of the target state, an observer maneuver is required. Thus, estimation of target state from bearing observations requires a minimum of two legs of data. This observability property of the dynamic process results in a piecewise convergence of the state estimate. It is this property that distinguishes the passive bearings-only problem from the more conventional target trackers and motion analysis systems.[3-7]

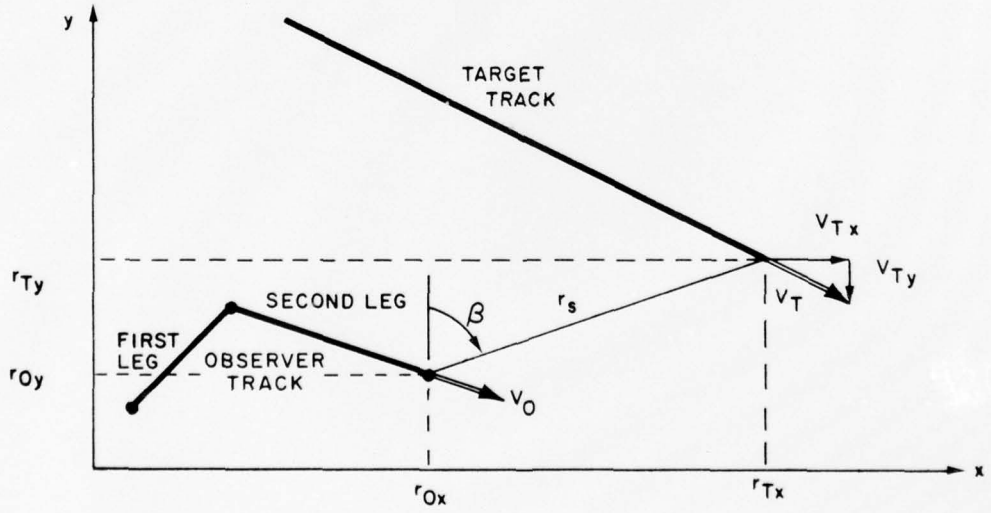

Figure 2. Special Case: All Bearing Measurements Generated by a Single Moving Observer

In the next section, a representation of the target-observer motion process that is inherently linear in form is developed; this departs from past efforts where linearization about the nominal or estimated target state is required. Determination of the target position and velocity is then directly derived from the application of linear estimation theory. Next, the properties of estimators for "piecewise observable" systems and the initialization of the recursive algorithm are examined in detail. The practical implementation of the motion analysis algorithm is then discussed, and experimental results are presented.

MODELING OF THE TARGET-OBSERVER DYNAMICS

A plot of the target and observer motion was shown in figure 2. The discrete-time equation for the target state assuming constant velocity is given by

$$x_T(k+1) = \begin{bmatrix} 1 & 0 & t_s & 0 \\ 0 & 1 & 0 & t_s \\ 0 & 0 & 1 & 0 \\ 0 & 0 & 0 & 1 \end{bmatrix} \quad x_T(k) = \Phi(k+1, k)x_T(k), \tag{1}$$

where t_s is the time increment between data samples, and $\Phi(k+1, k)$ is the discrete transition matrix. The observer motion is unrestricted and given by

$$\begin{bmatrix} r_{Ox}(k+1) \\ r_{Oy}(k+1) \end{bmatrix} = \begin{bmatrix} 1 & 0 \\ 0 & 1 \end{bmatrix} \begin{bmatrix} r_{Ox}(k) \\ r_{Oy}(k) \end{bmatrix} + t_s \begin{bmatrix} V_{Ox}(k) \\ V_{Oy}(k) \end{bmatrix}. \tag{2}$$

Equation (2) can be recast as

$$x_O(k+1) = \Phi(k+1, k)x_O(k) + \begin{bmatrix} 0 \\ \hline I \end{bmatrix} \begin{bmatrix} \Delta V_{Ox}(k) \\ \Delta V_{Oy}(k) \end{bmatrix}, \tag{3}$$

where

$$\Delta V_O(k) = V_O(k+1) - V_O(k) \tag{4}$$

is the incremental change in the observer velocity. The bearing to the target is defined by the relation

$$\tan \beta(k) = [r_{Tx}(k) - r_{Ox}(k)]/[r_{Ty}(k) - r_{Oy}(k)], \tag{5}$$

or, equivalently,

$$[r_{Tx}(k) - r_{Ox}(k)] \cos \beta(k) - [r_{Ty}(k) - r_{Oy}(k)] \sin \beta(k) = 0. \quad (6)$$

The bearing measurements viewed by the observer are noise corrupted; that is,

$$\beta_m(k) = \beta(k) + \nu(k), \quad (7)$$

where $\nu(k)$ is assumed to be a purely random sequence with zero mean and variance $\sigma_\nu^2(k)$. When the measured bearing is used in place of the true bearing in equation (6), this relationship becomes

$$\begin{aligned}
&[r_{Tx}(k) - r_{Ox}(k)] \cos \beta_m(k) - [r_{Ty}(k) - r_{Oy}(k)] \sin \beta_m(k) \\
&\quad = \{[r_{Tx}(k) - r_{Ox}(k)] \cos \beta(k) - [r_{Ty}(k) - r_{Oy}(k)] \sin \beta(k)\} \cos \nu(k) \\
&\qquad - \{[r_{Tx}(k) - r_{Ox}(k)] \sin \beta(k) + [r_{Ty}(k) - r_{Oy}(k)] \cos \beta(k)\} \sin \nu(k) \\
&\quad = - r_s(k) \sin \nu(k), \quad (8)
\end{aligned}$$

where the last step results from substituting equation (6) and identifying the quantity

$$r_s(k) = [r_{Tx}(k) - r_{Ox}(k)] \sin \beta(k) + [r_{Ty}(k) - r_{Oy}(k)] \cos \beta(k) \quad (9)$$

as the slant range between the target and the observer. Rearranging equation (8) to isolate the unknown quantities yields

$$\begin{aligned}
&r_{Ox}(k) \cos \beta_m(k) - r_{Oy}(k) \sin \beta_m(k) \\
&\qquad = r_{Tx}(k) \cos \beta_m(k) - r_{Ty}(k) \sin \beta_m(k) + r_s(k) \sin \nu(k), \quad (10)
\end{aligned}$$

where the left-hand side is available as a measurement. Defining

$$H(k) = H[\beta_m(k)] = [\cos \beta_m(k) \quad -\sin \beta_m(k) \quad 0 \quad 0] \quad (11)$$

and

$$z(k) = H(k) x_O(k) \quad (12)$$

as the measurement matrix and measurement equation, respectively, equation (10) assumes the compact form

$$z(k) = H(k) x_T(k) + \eta(k), \quad (13)$$

where the system dynamics are

$$x_T(k+1) = \Phi(k+1, k)x_T(k); \tag{14}$$

and where

$$\eta(k) = r_s(k) \sin \nu(k) \approx r_s(k)\, \nu(k) \tag{15}$$

represents the measurement noise. When the perturbations $\nu(k)$ are Gaussian, the statistics of $\eta(k)$ are

$$M_\eta(k) = \frac{1}{\sqrt{2\pi}\,\sigma_\nu} \int_{-\infty}^{\infty} r_s(k) \sin \nu \exp\left(-\frac{\nu^2}{2\sigma_\nu^2}\right) d\nu = 0, \tag{16a}$$

and

$$\sigma_\eta^2(k) = \frac{1}{\sqrt{2\pi}\,\sigma_\nu} \int_{-\infty}^{\infty} r_s^2(k) \sin^2 \nu(k) \exp\left(-\frac{\nu^2}{2\sigma_\nu^2}\right) d\nu$$

$$= \frac{1}{2} r_s^2(k) \left\{1 - \exp[-2\sigma_\nu^2(k)]\right\} \approx r_s^2(k)\sigma_\nu^2(k), \tag{16b}$$

where $M_\eta(k)$ and $\sigma_\eta^2(k)$ are the mean and variance of η, respectively. Thus, given equations (13), (14), (15), and (16), the problem of determining the target position and velocity (i.e., target state vector) from a history of noisy bearing measurements

$$Z(k) = [z(k)\ z(k-1) \ldots z(1)]' \tag{17}$$

has the form of a linear state estimation problem. The problem is complicated, however, by the fact that even for the noise-free situation the matrix pair $[\Phi, H(k)]$ is unobservable during the first leg. That is, the matrix

$$\sum_{i=1}^{k} [H(i)\Phi(i, k)]' \ [H(i)\Phi(i, k)]$$

is only positive semi-definite and does not achieve full rank until an observer maneuver occurs (see appendix A).

ESTIMATION OF TARGET STATES

The bearings-only motion analysis problem is stated as follows: Given the vector-valued random process $x(k)$ and observed random variables $Z(k) = [z(k)\ z(k-1) \ldots z(1)]'$, find an estimate $\hat{x}(k|k)$ that minimizes the expected loss $E\{L(\epsilon)\} = E\{L[||\hat{x}(k) - x(k)||]\}$. Under assumptions that are consistent with practical constraints and desired behavior, the optimal estimate is given by the conditional expectation[8]

$$\hat{x}(k|k) = E[x(k)|Z(k)]. \tag{18}$$

If the random processes are Gaussian, the conditional expectation is identical with the orthogonal projection of $x(k)$ on the measurement space.[9,10] However, if $L(\epsilon) = \epsilon^2$ and the estimates are restricted to be a linear combination of the measurement $Z(k)$, then the optimal estimate is also the orthogonal projection. Thus, linear estimation is bettered by nonlinear estimation only if the random processes are non-Gaussian and then only if third-order and higher probability distributions are considered.[8] For the bearings-only motion analysis problem, $\nu(k)$ is generally assumed Gaussian, and the near equality of equation (15) holds for typical noise environments; thus, linear estimation yields the optimal estimate for essentially all performance criteria. A unified treatment on the theory of linear estimation is now presented.

LINEAR ESTIMATION

Given the dynamic system

$$x(k+1) = \Phi(k+1, k)x(k) \tag{19}$$

and measurement equation

$$z(k) = H(k)x(k) + \eta(k), \tag{20}$$

the vector $Z(k)$ of equation (17) can be written as

$$Z(k) = A(k)x(k) + N(k), \tag{21}$$

where

$$A(k) = \begin{bmatrix} H(k) \\ H(k-1)[\Phi(k-1, k)] \\ \vdots \\ H(1)[\Phi(1, k)] \end{bmatrix} \tag{22}$$

and

$$N(k) = [\eta(k)\ \eta(k-1) \ldots \eta(1)]'. \tag{23}$$

The penalty or loss assigned to state error defined by

$$\begin{aligned} L &= E\{||x(k) - \hat{x}(k|k)||^2\} \\ &= \mathrm{tr}E\{[x(k) - \hat{x}(k|k)]\ [x(k) - \hat{x}(k|k]'\} \\ &= \mathrm{tr}P(k) \end{aligned} \tag{24}$$

serves as a measure of the quality of the estimate, where $\mathrm{tr}[\cdot]$ denotes the trace of the matrix and $P(k)$ is the error covariance matrix. This loss function is minimized when the state error $[x(k) - \hat{x}(k|k)]$ is orthogonal to the available data; that is,

$$E\{[x(k) - \hat{x}(k|k)]\ Z'(k)\} = [0] = \text{null matrix}. \tag{25}$$

The state estimate assumes the form

$$\hat{x}(k|k) = B(k)Z(k), \tag{26}$$

where the linear combination of the measurements defined by the matrix $B(k)$ is to be determined. Substituting equations (21) and (26) into equation (25) yields

$$P_x(k)A'(k) - B(k)[A(k)P_x(k)A'(k) + R(k)] = [0], \tag{27}$$

where

$$R(k) = E[N(k)N'(k)]$$

$$= \begin{bmatrix} \sigma_\eta^2(k) & 0 & \cdot & \cdot & \cdot & 0 \\ 0 & \sigma_\eta^2(k-1) & 0 & \cdot & \cdot & \cdot \\ \cdot & 0 & \cdot & & & \cdot \\ \cdot & \cdot & & \cdot & & \cdot \\ \cdot & \cdot & & & \cdot & 0 \\ 0 & \cdot & \cdot & \cdot & 0 & \sigma_\eta^2(1) \end{bmatrix} \tag{28}$$

and where

$$P_x(k) = E[x(k)x'(k)] = \Phi(k, 0)P_x(0)\Phi'(k, 0) \tag{29}$$

is the covariance matrix of $x(k)$ without any measurement, and $P_x(0)$ is the a priori covariance of the unknown vector or state. From equation (27), the optimal value for the matrix $B(k)$ is

$$\begin{aligned} B(k) &= P_x(k)A'(k)[R(k) + A(k)P_x(k)A'(k)]^{-1} \\ &= [P_x^{-1}(k) + A'(k)R^{-1}(k)A(k)]^{-1}A'(k)R^{-1}(k), \end{aligned} \tag{30}$$

where the last step results from the matrix inversion identity of equation (B-1) presented in appendix B. Note that, if $P_x(o) = \sigma_0^2 I$ and $R = [0]$—or, equivalently, R is finite and $P_x(o) = \lim_{\sigma^2 \to \infty} \sigma_0^2 I$, then

$$B(k) = A'(k)[A(k)A'(k)]^{-1} \tag{31}$$

is the pseudoinverse of $A(k)$ yielding a minimum norm solution for the unknown $x(k)$ for the underdetermined case (fewer equations or measurements than unknowns).[10,11] When the number of measurements exceeds the number of unknowns, the inverse in equation (31) no longer exists and one is forced to edit the number of measurements to achieve a compatible system. If noise is present ($R \neq [0]$), the identity in equation (30) holds and all the measurements may be employed in extracting the estimates. Note that, if $P_x^{-1} = [0]$, implying no a priori information, the relation

$$B(k) = [A'(k)R^{-1}(k)A(k)]^{-1}A'(k)R^{-1}(k) \tag{32}$$

results, which yields the weighted least-squares solution for the overdetermined case (more measurements than unknowns).[10,11] The transition between cases is given by the general form of equation (30), which based on equations (21) and (26), represents a "generalized" inverse of the matrix $A(k)$. (The relationship of $B(k)$ to the standard generalized inverse or pseudoinverse, and sequential estimation via the Kalman algorithm is treated in the next section.)

With the optimal estimator defined by equations (26) and (30), the error covariance matrix in equation (24) becomes

$$\begin{aligned} P(k|k) &= P_x(k) - B(k)A(k)P_x(k) \\ &= P_x(k) - P_x(k)A'(k)[R(k) + A(k)P_x(k)A'(k)]^{-1}A(k)P_x(k), \end{aligned} \tag{33}$$

where the first step utilizes the fact that the optimal value of x is orthogonal to the state error and $E\{[x-\hat{x}][x-\hat{x}]'\} = E\{(x-\hat{x})x'\}$. By use of the matrix inversion lemma equation (B-2)—appendix B, the optimal error covariance matrix becomes

$$P(k|k) = [P_x^{-1}(k) + A'(k)R^{-1}(k)A(k)]^{-1}. \tag{34}$$

Combining equations (34), (30), and (26) yields as the optimal estimate

$$\hat{x}(k|k) = P(k)A'(k)R^{-1}(k)Z(k). \tag{35}$$

The updating of the state estimate $\hat{x}(k|k)$, and its measure of quality $P(k|k)$, as new measurements become available is efficiently accomplished by a recursive algorithm. Recasting equation (34) in the form

$$P^{-1}(k|k) = P_x^{-1}(k) + A'(k)R^{-1}(k)A(k), \tag{36}$$

utilizing equations (22), (28), and (29), and noting that

$$A(k+1) = \begin{bmatrix} H(k+1) \\ \hline A(k)\Phi(k, k+1) \end{bmatrix}$$

permits the updating of the error covariance matrix to be expressed in the form

$$\begin{aligned} P^{-1}(k+1|k+1) = {} & [\Phi(k+1,k)P_x(k)\Phi'(k+1,k)]^{-1} \\ & + [\Phi^{-1}(k+1,k)]'A'(k)R^{-1}(k)A(k)\Phi^{-1}(k+1,k) \\ & + \frac{1}{\sigma_\eta^2(k+1)} H'(k+1)H(k+1) \\ = {} & [\Phi'(k+1,k)]^{-1}[P_x^{-1}(k) + A'(k)R^{-1}(k)A(k)]\Phi^{-1}(k+1,k) \\ & + \frac{1}{\sigma_\eta^2(k+1)} H'(k+1)H(k+1). \end{aligned} \tag{37}$$

Substituting equation (34) into equation (37) and invoking the matrix inversion lemma (equation (B-2)) yields the computational convenient form

$$\begin{aligned} P(k+1|k+1) = {} & P(k+1|k) - P(k+1|k)H'(k+1) \\ & \cdot [H(k+1)P(k+1|k)H'(k+1) + \sigma_\eta^2(k+1)]^{-1} \\ & \cdot H(k+1)P(k+1|k), \end{aligned} \tag{38}$$

where

$$P(k+1|k) = \Phi(k+1,k)P(k|k)\Phi'(k+1,k). \tag{39}$$

Equation (39) represents the predicted value of the covariance matrix, and equation (38), the corrected or updated value. Note that by direct expansion of equation (36) it can be shown that

$$P^{-1}(k|k) = \{\Phi(k,0)P_x(0)\ [\Phi'(k,0)]\}^{-1} + \sum_{i=1}^{k} \frac{1}{\sigma_\eta^2(i)} \{[H(i)\Phi(i,k)]'\}\ \{[H(i)\Phi(i,k)]\}. \tag{40}$$

Observability assumes that the second term of equation (40) is positive definite. However, as noted earlier for the single moving observer bearings-only motion analysis problem, the observability of the matrix depends upon whether or not an observer maneuver has occurred. This behavior and the problem of initializing the covariance matrix are detailed in the next section.

From equation (35) the updated state estimate following a new measurement is given by

$$\begin{aligned} x(k+1|k+1) &= P(k+1|k+1)A'(k+1)R^{-1}(k+1)Z(k+1) \\ &= P(k+1)|k+1)[H'(k+1)\,\vdots\,\Phi'(k-1,k)A'(k)] \\ &\quad \cdot \left[\begin{array}{c:c} \sigma_\eta^2(k+1) & 0 \\ \hdashline 0 & R(k) \end{array}\right] \left[\begin{array}{c} z(k+1) \\ \\ Z(k) \end{array}\right]. \end{aligned} \tag{41}$$

After some manipulation, the substitution of equation (38) into equation (41) yields

$$\hat{x}(k+1|k+1) = \hat{x}(k+1|k) + K(k+1)[z(k+1) - H(k+1)\hat{x}(k+1|k)], \tag{42}$$

where

$$\hat{x}(k+1|k) = \Phi(k+1,k)\hat{x}(k|k) \tag{43}$$

is the predicted target state, and the correction based on the latest measurement is applied with gain

$$K(k+1) = P(k+1|k)H'(k+1)[H(k+1)P(k+1|k)H'(k+1) + \sigma_\eta^2(k+1)]^{-1}. \tag{44}$$

Equations (38), (39), (42), (43), and (44) are the Kalman-Bucy filter equations.[12] This link between regressive least squares and Kalman filtering for observable systems was established earlier by Bryson and Ho[13] and Fagin[14].

PROPERTIES OF LINEAR ESTIMATORS AND INITIALIZATION OF THE RECURSIVE ALGORITHM

Given the set of simultaneous linear equations

$$Z(k) = A(k)x(k) + N(k), \tag{21}$$

where without loss of generality it is assumed that the data are normalized such that $E[NN'] = \sigma^2 I$, the general solution is classically given by[15]

$$\hat{x}_{LS}(k) = A^{\#}(k)Z(k) + [I - A^{\#}(k)A(k)]W. \tag{45}$$

The matrix $A^{\#}(k)$ is the pseudoinverse of the matrix $A(k)$, and W is an arbitrary vector.[15] The pseudoinverse of $A(k)$ is defined by

$$A^{\#}(k) = [A'(k)A(k)]^{-1}A'(k) \tag{46}$$

when $A'(k)A(k)$ is of full rank, and by

$$A^{\#}(k) = [A'(k)A(k)]^{\#}A'(k) \tag{47}$$

when the system is unobservable. Since $A'(k)A(k)$ is symmetric, an orthogonal transformation T exists such that

$$A'(k)A(k) = T\Lambda T', \tag{48}$$

where

$$\Lambda = \begin{bmatrix} \lambda_1 & 0 & 0 & \cdots & \cdots & \cdots & 0 \\ 0 & \lambda_2 & 0 & \cdots & \cdots & \cdots & 0 \\ 0 & 0 & \ddots & & & \cdots & \cdots \\ \cdots & \cdots & \cdots & \lambda_{n-q_A} & \cdots & \cdots & \cdots \\ \cdots & \cdots & \cdots & & 0 & \cdots & \cdots \\ \cdots & \cdots & \cdots & \cdots & \cdots & \ddots & \\ 0 & 0 & \cdots & \cdots & \cdots & \cdots & 0 \end{bmatrix}$$

$$= \left[\begin{array}{c|c} \mathrm{diag}[\lambda_i] & [0] \\ \hline [0] & [0] \end{array}\right] \tag{49}$$

where n is the number of states and q_A is the degeneracy of $A'(k)A(k)$. Thus, the pseudoinverse of a symmetric matrix is defined by

$$[A'(k)A(k)]^{\#} = T\Lambda^{\#}T'$$

$$= T\begin{bmatrix} \operatorname{diag}\left[\frac{1}{\lambda_i}\right] & [0] \\ [0] & [0] \end{bmatrix} T'. \qquad (50)$$

The value of $\hat{x}$ given by equation (45) represents the best estimate, in a weighted least-squares sense, to equation (21). This solution is unique when $A'(k)A(k)$ is nonsingular since, by equation (46), the second term in equation (45) vanishes. When the process is unobservable, that is

$$\det[A'(k)A(k)] = \det \sum_{i=1}^{k} [H(i)\,\Phi(i,k)]'[H(i)\,\Phi(i,k)] = 0, \qquad (51)$$

a (q_A) parameter family of solutions for $x(k)$ exists. However, even in this case, particular types of solutions can be singled out by imposing additional constraints. A common selection, from the infinity of solutions, is that of the minimum norm. Since the two vectors comprising the right-hand side of equation (45) are orthogonal,[10,15] the minimum norm solution occurs when $W = [0]$, and is given by

$$x(k) = A^{\#}(k)Z(k). \qquad (52)$$

In the motion analysis problem for the relative target state $x_R = x_T - x_O$, this solution (i.e., equation (52)) yields the null vector during the entire first phase (leg). However, under these conditions, a range-normalized solution is often sought. From the foregoing discussions, it is clear that such a relative motion solution must be derived from the second term in equation (45).

To compute $\hat{x}_{LS}(k)$ sequentially, one employs

$$\hat{x}_{LS}(k) = P_{LS}(k)A'(k)Z(k), \qquad (53)$$

where, in this case,

$$P_{LS}(k) = [A'(k)A(k)]^{\#}. \qquad (54)$$

As with the processing of equation (34) in the preceding section, use of the matrix inversion lemma is the key to the sequential updating of $\hat{x}(k\,|\,k)$ as new measurements become available. However, until the number of measurements equals the number of states and during the entire first leg of the single moving observer problem the process is not observable and $A'(k)A(k)$ is singular.

Under these conditions, algorithms capable of generating the exact pseudoinverses are given by Cline.[16] However, in this report, consideration is given to the use of a positive matrix $P_x(k|0)$ in computing the inverse, that is, approximate $P_{LS}(k)$ in equation (54) by

$$P(k|k) = \hat{P}_{LS}(k) = [P_x(k|0)^{-1} + A'(k)A(k)]^{-1}$$

$$= \Phi(k,0)[P^{-1}(0|0) + \Phi'(k,0)A'(k)A(k)\Phi(k,0)]^{-1}\Phi'(k,0), \qquad (55)$$

where $P(0|0)$ is large. Note that this form for $P(k|k)$ is directly achieved in the development presented in the preceding section and results in the standard Kalman computation, with $P(0|0)$ representing the initial error covariance matrix. The effect of $P(0|0)$ on the computation of $P(k)$ for the specific choice

$$P(0|0) = \sigma_0^2 I \qquad (56)$$

is now examined.

Substituting equation (56) into equation (55) yields

$$P(k|k) = \Phi(k,0)\left[\frac{1}{\sigma_0^2} I + A_1'(k)A_1(k)\right]\Phi'(k,0), \qquad (57)$$

where $A_1(k) = A(k)\Phi(k,0)$. Since $A_1'(k)A_1(k)$ is symmetric, an orthogonal transformation T_1 exists such that

$$P^{\#}_{LS_1}(k) = A_1'(k)A_1(k) = T_1\Omega_1 T_1', \qquad (58)$$

where

$$\Omega_1 = \begin{bmatrix} \overline{\text{diag}[\omega_i]} & \vdots & \overline{[0]} \\ - - - - - & \vdots & - - - - \\ [0] & \vdots & [0] \end{bmatrix}, \quad i = 1, 2, \ldots, n - q_A.$$

Substituting equation (58) into equation (57) yields

$$P(k|k) = \Phi(k,0)\, T_1 \left[\frac{1}{\sigma_0^2} I + \Omega_1\right]^{-1} T_1' \Phi'(k,0)$$

$$= \Phi(k,0)\, T_1 \left[\begin{array}{c|c} \operatorname{diag}\left[\dfrac{1}{\sigma_0^2} + \omega_i\right] & [0] \\ \hline [0] & \dfrac{1}{\sigma_0^2} I \end{array}\right]^{-1} T_1' \Phi'(k,0)$$

$$= \Phi(k,0)\, T_1 \left[\begin{array}{c|c} \operatorname{diag} \dfrac{1}{\omega_i + \sigma_0^2} & [0] \\ \hline [0] & \sigma_0^2 I \end{array}\right] T_1' \Phi'(k,0). \quad (59a)$$

Separating the observable and unobservable components of $P(k|k)$ permits equation (59a) to be recast as

$$P(k|k) = \Phi(k,0)\, T_1 \left[\begin{array}{c|c} \operatorname{diag}\left[\dfrac{1}{\omega_i + \dfrac{1}{\sigma_0^2}}\right] & [0] \\ \hline [0] & [0] \end{array}\right] T_1' \Phi'(k,0)$$

$$+ \sigma_0^2\, \Phi(k,0)\, T_1 \left[\begin{array}{c|c} I - \begin{pmatrix} I_{n-q_A} & [0] \\ \hline [0] & [0] \end{pmatrix} \end{array}\right] T_1' \Phi'(k,0). \quad (59b)$$

Since

$$\operatorname{diag}\left[\frac{1}{\omega_i + \dfrac{1}{\sigma_0^2}}\right] = \operatorname{diag}\left\{\frac{1}{\omega_i} - \frac{1}{\sigma_0^2\, \omega_i}\left[\frac{1}{\omega_i + \dfrac{1}{\sigma_0^2}}\right]\right\},$$

it follows that

$$P(k|k) = \Phi(k,0)\Phi'(k,0)\left[\Phi(k,0)\Phi'(k,0) + \frac{1}{\sigma_0^2} P_{LS}(k)\right]^{-1} P_{LS}(k)$$

$$+ \sigma_0^2 \Phi(k,0)\Phi'(k,0)\left[I - P_{LS}^{\#}(k) P_{LS}(k)\right],$$

$$= P_{LS}(k) - \frac{1}{\sigma_0^2} P_{LS}\left[\Phi(k,0)\Phi'(k,0) + \frac{1}{\sigma_0^2} P_{LS}(k)\right]^{-1} P_{LS}(k)$$

$$+ \sigma_0^2 \Phi(k,0)\Phi'(k,0)\left[I - A^{\#}(k) A(k)\right]. \qquad (60)$$

Substituting equation (60) into equation (53) shows that the measurements are indeed processed by a matrix that approximates $A^{\#}(k)$. Specifically,

$$P(k|k)A'(k) = \tilde{A}^{\#}(k) = A^{\#}(k) - \frac{1}{\sigma_0^2} P_{LS}(k)\left[\Phi(k,0)\Phi'(k,0) + \frac{1}{\sigma_0^2} P_{LS}(k)\right]^{-1} A^{\#}(k), \qquad (61)$$

where use of the identity $A^{\#}AA' = A'$ has been made. Thus, the introduction of an appropriate nonsingular $P(0|0)$ (specifically, $P(0|0) = \sigma_0^2 I$ as detailed above) permits the standard recursive algorithm to be employed in the calculation of the pseudoinverse matrix $\tilde{A}^{\#}(k)$. The second term in equation (60) has no effect on either the estimates or the Kalman gain since

$$P(k|k)H'(k) = \Phi(k,0)\Phi'(k,0)\left[\Phi(k,0)\Phi'(k,0) + \frac{1}{\sigma_0^2} P_{LS}(k)\right]^{-1} P_{LS}(k)H'(k).$$

The effect of $P(0|0)$ on the estimates clearly depends on how closely $\tilde{A}^{\#}$ approximates $A^{\#}$. As a cautionary note, it should be pointed out that in selecting values for σ_0^2 for initializing the computation of $P(k)$, the choice of an overly large value results in computational difficulties since the recursion formulas involve the differencing of large quantities.

The optimal state estimate is defined by equation (42), which upon regrouping of the terms becomes

$$\hat{x}(k+1|k+1) = [I - K(k+1)H(k+1)]\Phi(k+1,k)\,\hat{x}(k|k) + K(k+1)z(k+1). \qquad (62)$$

The general solution to equation (62) is

$$\hat{x}(k|k) = \phi(k,0)\hat{x}(0|0) + \sum_{j=1}^{k} \phi(k,j)K(j)z(j), \tag{63a}$$

where

$$\phi(k+1,k) = [I - K(k+1)H(k+1)]\Phi(k+1,k). \tag{63b}$$

It is shown in appendix C that

$$\sum_{j=1}^{k} \phi(k,j)K(j)z(j) = \tilde{A}^{\#}(k)Z(k),$$

$$\phi(k,0) = [I - \tilde{A}^{\#}(k)A(k)]\Phi(k,0),$$

which allows equation (63a) to be recast as

$$\hat{x}(k|k) = \tilde{A}^{\#}(k)Z(k) + [I - \tilde{A}^{\#}(k)A(k)]\hat{x}(k|0). \tag{64}$$

Thus, when the process is unobservable, the minimum norm solution is realized by initializing the recursive algorithm with $\hat{x}(0|0) = [0]$. To obtain other solutions, such as the range-normalized solution during the first leg of the single moving observer problem, requires an appropriate selection of $\hat{x}(0|0)$.

The relationship of the estimate $x(k|k)$ with the classical least-squares solution can be established by substituting equation (61) into equation (64) and utilizing equation (45), where $W = \hat{x}(k|0)$. Specifically,

$$\hat{x}(k|k) = \hat{x}_{LS}(k) - \frac{1}{\sigma^2} P_{LS}(k)[\Phi(k,0)\Phi'(k,0) + \frac{1}{\sigma^2} P_{LS}(k)]^{-1}[\hat{x}_{LS}(k) - \hat{x}(k|0)], \tag{65}$$

where for observable systems $\lim_{k\to\infty} P_{LS}(k) = [0]$ and $A^{\#}(k)A(k) = I$. Thus, the estimate of the Kalman-style algorithm asymptotically yields the pseudo-inverse solution.

APPLICATION TO THE MOTION ANALYSIS PROBLEM

This section is concerned with various state representations for the motion analysis problem and the resulting estimation algorithms. For the target state x_T, the results of the preceding section apply directly and the estimate is given by

$$\hat{x}_T(k+1|k+1) = \hat{x}_T(k+1|k) + K(k+1)[z(k+1) - H(k+1)\hat{x}_T(k+1|k)] , \tag{66}$$

where

$$\hat{x}_T(k+1|k) = \Phi(k+1,k)\hat{x}_T(k|k).$$

This representation is preferred for the general problem of multiple observers. However, for the single moving observer problem, the relative target state

$$x_R = x_T - x_O = \begin{bmatrix} r_x(k) \\ r_y(k) \\ V_x(k) \\ V_y(k) \end{bmatrix}$$

is often of interest and equation (42) reduces to

$$\begin{aligned} \hat{x}_R(k+1|k+1) &= \hat{x}_R(k+1|k) + K(k+1)[H(k+1)x_O(k+1) - H(k+1)\hat{x}_T(k+1|k)] \\ &= \hat{x}_R(k+1|k) - K(k+1)H(k+1)\hat{x}_R(k+1|k), \end{aligned} \tag{67a}$$

where the predicted state is given by

$$\hat{x}_R(k+1|k) = \Phi(k+1,k)\hat{x}_R(k|k) - \begin{bmatrix} 0 \\ \cdots \\ I \end{bmatrix} \Delta V_O(k). \tag{67b}$$

The estimated target velocity vector $\hat{V}_T(k+1|k+1)$ can be obtained by adding observer velocity components to $\hat{V}_x(k+1|k+1)$ and $\hat{V}_y(k+1|k+1)$; that is,

$$\begin{bmatrix} \hat{V}_{Tx}(k+1|k+1) \\ \hat{V}_{Ty}(k+1|k+1) \end{bmatrix} = \begin{bmatrix} \hat{V}_x(k+1|k+1) \\ \hat{V}_y(k+1|k+1) \end{bmatrix} + \begin{bmatrix} \hat{V}_{Ox}(k+1) \\ \hat{V}_{Oy}(k+1) \end{bmatrix} . \tag{68}$$

The relationship between the various estimates is illustrated in figures 3a through 3c, where the covariance and gain matrices are generated via equations (38) and (44), respectively. The recursive estimation of the relative target state $x_R(k)$ is summarized in table 1.

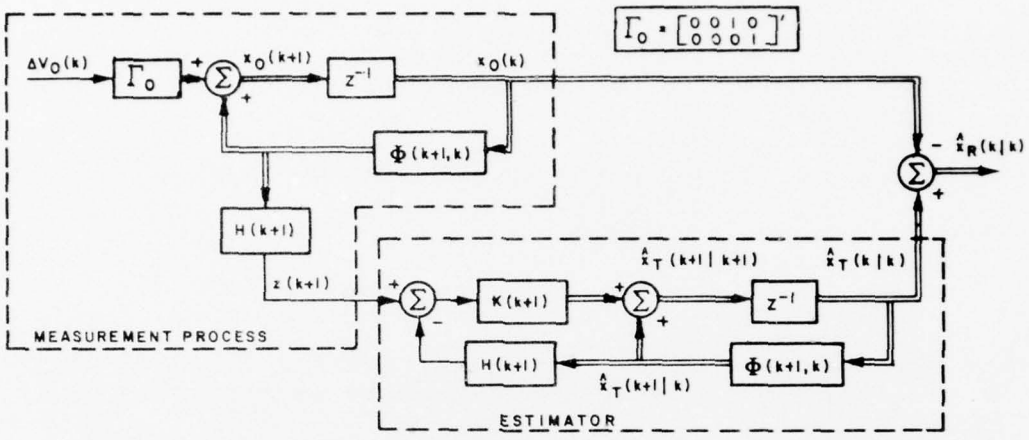

Figure 3a. Block Diagram of Observer Dynamics, Measurement Equation, and Estimator for Unknown Target State $x_T(k)$ (Also Shown is Relative Target State $x_R(k) = x_T(k) - x_O(k)$)

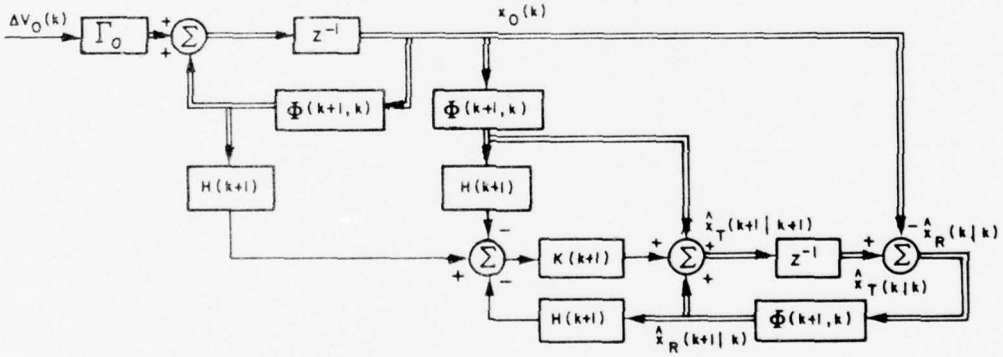

Figure 3b. Equivalent Block Diagram of Figure 3a

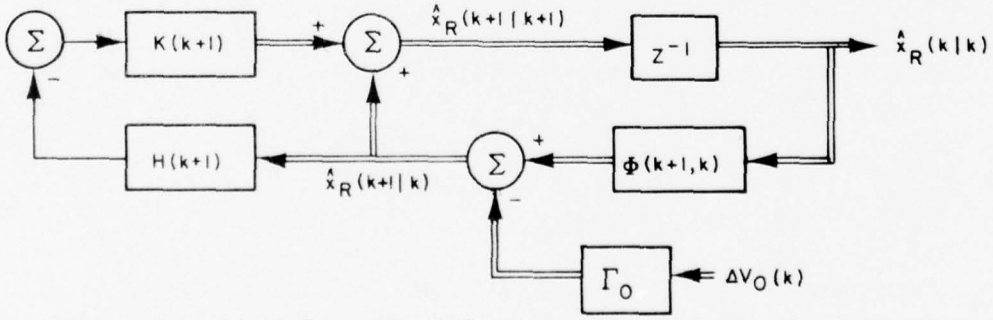

Figure 3c. Block Diagram of Estimator for $x_R(k)$ Resulting from Simplification of Figure 3b

Table 1. Summary of the Recursive Estimation of the Relative Target State $x_R(k)$

State Vector:

$$x_R(k) = [r_x(k) \quad r_y(k) \quad V_x(k) \quad V_y(k)]' \tag{1-1}$$

Initialization:*

$$\hat{x}_R(0|0) = [\hat{r}_s(0) \sin\beta_m(0) \quad \hat{r}_s(0) \cos\beta_m(0) \quad 0 \quad 0]' \tag{1-2}$$

$$P(0|0) = \sigma_0^2 I, \text{ where } \sigma_0^2 = \text{constant} \tag{1-3}$$

Predicted State:

$$\hat{x}_R(k+1|k) = \Phi(k+1,k)\hat{x}_R(k|k) - \begin{bmatrix} 0 & 0 & 1 & 0 \\ 0 & 0 & 0 & 1 \end{bmatrix}' \Delta V_O(k) \tag{1-4}$$

Predicted Covariance Matrix:

$$P(k+1|k) = \Phi(k+1,k)P(k|k)\Phi'(k+1,k) \tag{1-5}$$

Measurement Matrix:

$$H(k+1) = [\cos\beta_m(k+1) \quad -\sin\beta_m(k+1) \quad 0 \quad 0] \tag{1-6}$$

Gain Matrix Computation:

$$K(k+1) = P(k+1|k)H'(k+1)[H(k+1)P(k+1|k)H'(k+1) + r_s^2(k+1)\sigma_\nu^2(k+1)]^{-1} \tag{1-7}$$

Updated State:

$$\hat{x}_R(k+1|k+1) = \hat{x}_R(k+1|k) - K(k+1)H(k+1)\hat{x}_R(k+1|k) \tag{1-8}$$

Updated Covariance Matrix:

$$P(k+1|k+1) = [I - K(k+1)H(k+1)]P(k+1|k) \tag{1-9}$$

Target Parameters:

$$\hat{r}_s(k+1|k+1) = [\hat{r}_x^2(k+1|k+1) + \hat{r}_y^2(k+1|k+1)]^{1/2} \tag{1-10}$$

$$\hat{C}_T(k+1|k+1) = \tan^{-1}[\hat{V}_{Tx}(k+1|k+1)/\hat{V}_{Ty}(k+1|k+1]^{1/2} \tag{1-11}$$

$$\hat{S}_T(k+1|k+1) = [\hat{V}_{Tx}^2(k+1|k+1) + \hat{V}_{Ty}^2(k+1|k+1)]^{1/2} \tag{1-12}$$

$$\hat{\beta}(k+1|k+1) = \tan^{-1}[\hat{r}_x(k+1|k+1)/\hat{r}_y(k+1|k+1)] \tag{1-13}$$

*Initialization is discussed in the next section.

IMPLEMENTATION OF THE SINGLE OBSERVER TMA ALGORITHM

The computation of the gain and covariance matrix in table 1 requires knowledge of the slant range $r_S(k)$, which is initially unknown to the observer. However, from equations (52) and (53) it should be noted that lack of knowledge of the noise variance

$$\sigma_\eta^2(k) \approx r_s^2(k)\sigma_\nu^2(k)$$

in the computation of $P(k)$ does not preclude achieving an estimate. For example, if the noise variance is assumed stationary, representing equal weight on all data, a least-squares estimate results. Since the role of the noise variance in the computations is to assign a weight to each measurement, a near-optimal implementation can be realized when the range is slowly varying by assigning a constant value for $r_S(k)$. Introducing the normalized covariance matrix $P_N(k|k)$ such that

$$P(k|k) = r_s^2(k)P_N(k|k) \tag{69}$$

permits equations (1-5) and (1-9) to assume the normalized form

$$P_N(k+1|k+1) = \frac{r_s^2(k)}{r_s^2(k+1)}\left[P_N(k+1|k) - \frac{P_N(k+1|k)H'(k+1)H(k+1)P_N(k+1|k)}{H(k+1)P_N(k+1|k)H'(k+1)+\sigma_\nu^2(k+1)}\right]$$

$$\approx P_N(k+1|k) - \frac{P_N(k+1|k)H'(k+1)H(k+1)P_N(k+1|k)}{H(k+1)P_N(k+1|k)H'(k+1)+\sigma_\nu^2(k+1)}\ , \tag{70}$$

where

$$P_N(k+1|k) = \Phi(k+1,k)P_N(k|k)\Phi(k+1,k),$$

and where σ_ν^2 is the variance of the noise perturbing the bearing measurements, and the last step in equation (70) is approximately satisfied for slowly varying $r_S(k)$. Similarly, for the gain matrix, substitution of equation (69) into equation (1-7) yields

$$K(k+1) = \frac{P_N(k+1|k)H'(k+1)}{H(k+1)P_N(k+1|k)H'(k+1)+\sigma_\nu^2(k+1)} \tag{71}$$

Thus, the computation of both $P(k+1|k)$ and $K(k+1)$ is independent of target range when $P_N(0|0)$ is chosen independent of $r_s(0)$.

In the initialization of the state vector, it is seen from equation (65) that imposing a minimum norm solution on the relative target state $x_R = x_T - x_O$ (i.e., setting $\hat{x}_R(0|0) = [0]$) results in the trivial solution $\hat{x}_R(k|k) = [0]$ for all k on the first leg. To generate a relative motion (range-normalized) solution, it is observed from equation (1-8) that the gain matrix operates on the "estimated" cross-range residual; that is,

$$\begin{aligned} H(k)\hat{x}_R(k+1|k) &= \hat{r}_x(k+1|k)\cos[\beta(k+1) + \nu(k+1)] - \hat{r}_y(k+1|k)\sin[\beta(k+1) + \nu(k+1)] \\ &= -\hat{r}(k+1|k)\sin[\beta(k+1) - \hat{\beta}(k+1|k) + \nu(k+1)] \\ &= -\hat{r}(k+1|k)\sin[\Delta\beta(k+1) + \nu(k+1)]. \end{aligned} \tag{72}$$

Thus, if in the initial state estimate the relative velocity is zero, the solution for $\hat{x}_R(k)$ is proportional to (or scaled by) the initial slant range estimate. This is a desirable characteristic for the estimator, and the initialization of the state estimate given by

$$\hat{x}_R(0|0) = \begin{bmatrix} \hat{r}_s(0)\sin\beta_m(0) \\ \hat{r}_s(0)\cos\beta_m(0) \\ 0 \\ 0 \end{bmatrix} \tag{73}$$

is used in this report. On the second leg, the system becomes observable; thus, the second term in equation (45) fades and the significance of the initial value for $\hat{x}_R$ diminishes. In the initialization of the covariance matrix, experimental studies have shown that the choice

$$P(0|0) = \sigma_0^2 I, \tag{74}$$

where $\sigma_0^2 = r_s^2(0)$, produces good results in realizing the desired estimator performance. From equation (69) it is seen that setting $\sigma_0^2 = r_s^2(0)$ is equivalent to initializing

$$P_N(0|0) = I. \tag{75}$$

This initialization can be shown to generate weights on new data in a manner that takes into account the size of the bearing change between samples in relation to the bearing error due to measurement noise.[17] The normalized algorithm, including initialization, is summarized in table 2.

Table 2. Summary of the Normalized Recursive Algorithm

State Vector:

$$x_R(k) = [r_x(k) \quad r_y(k) \quad V_x(k) \quad V_y(k)]' \tag{2-1}$$

Initialization:

$$\hat{x}_R(0|0) = [\hat{r}_s(0) \sin\beta_m(0) \quad \hat{r}_s(0) \cos\beta_m(0) \quad 0 \quad 0]' \tag{2-2}$$

$$P_N(0|0) = I \tag{2-3}$$

Predicted Estimate:

$$\hat{x}_R(k+1|k) = \Phi(k+1,k)\hat{x}_R(k|k) - \begin{bmatrix} 0 & 0 & 1 & 0 \\ 0 & 0 & 0 & 1 \end{bmatrix}' \Delta V_O(k) \tag{2-4}$$

Predicted Covariance Matrix:

$$P_N(k+1|k) = \Phi(k+1,k)P_N(k|k)\Phi'(k+1,k) \tag{2-5}$$

Measurement Matrix:

$$H(k+1) = [\cos\beta_m(k+1) \quad -\sin\beta_m(k+1) \quad 0 \quad 0] \tag{2-6}$$

Gain Matrix Computation:

$$K(k+1) = P_N(k+1|k)H'(k+1)[H(k+1)P_N(k+1|k)H'(k+1) + \sigma_\nu^2(k+1)]^{-1} \tag{2-7}$$

Updated State:

$$\hat{x}_R(k+1|k+1) = \hat{x}_R(k+1|k) - K(k+1)H(k+1)\hat{x}_R(k+1) \tag{2-8}$$

Updated Covariance Matrix:

$$P_N(k+1|k+1) = [I - K(k+1)H(k+1)]P_N(k+1|k) \tag{2-9}$$

Target Parameters:

$$\hat{r}_s(k+1|k+1) = [\hat{r}_x^2(k+1|k+1) + \hat{r}_y^2(k+1|k+1)]^{1/2} \tag{2-10}$$

$$\hat{C}_T(k+1|k+1) = \tan^{-1}[\hat{V}_{Tx}(k+1|k+1)/\hat{V}_{Ty}(k+1|k+1)] \tag{2-11}$$

$$\hat{S}_T(k+1|k+1) = [\hat{V}_{Tx}^2(k+1|k+1) + \hat{V}_{Ty}^2(k+1|k+1)]^{1/2} \tag{2-12}$$

$$\hat{\beta}(k+1|k+1) = \tan^{-1}[\hat{r}_x(k+1|k+1)/\hat{r}_y(k+1|k+1)] \tag{2-13}$$

PROPERTIES OF THE TMA SOLUTION

The convergence of the recursive solution (Kalman) to the least-squares estimate as the number of measurements increases — see equation (65) — permits the behavior of the linear TMA estimator to be discussed in terms of the idealized estimate of equation (45). Note that the measurement matrix A(k), defined by equation (22), is a function of the measured bearing and hence the measurement noise $\nu(k)$. It is shown in appendix A that under noise-free conditions A'(k)A(k) is singular over the entire first leg. Since for the TMA problem the minimum norm solution $\hat{x}(k) = A^{\#}Z(k)$ is the null vector, the first leg solution prior to an observer maneuver must be the second term of equation (45). This represents the range-normalized solution.

In the experiments described in the next section this solution is indeed observed under low-noise conditions. However, when the level of the measurement noise is substantial, A'(k)A(k) becomes nonsingular even on the first leg; and hence the factor $[I - A^{\#}(k)A(k)]$ in equation (45) vanishes and the solution for any initial conditions collapses toward the minimum norm solution. This behavior appears to be abated in the low-noise case by preprocessing of the data and approximate computation of $A^{\#}(k)$. To demonstrate the consistency of the first leg behavior when A'(k)A(k) is nonsingular, i.e., to show that the addition of noise to the matrix A(k) *does not alter system observability*, recall that the measurements are generated from the measured bearings and observer position by equation (12); that is

$$z(k) = H(k)x_O(k) = H(k)x_T(k) + \eta(k).$$

On the first leg,

$$Z(k) = [z(k),\ z(k-1),\ \ldots,\ z(1)]' = A(k)x_O(k), \tag{76}$$

since observer velocity is constant. Consequently, the estimate is given by

$$\begin{aligned}\hat{x}(k|k) &= \tilde{A}^{\#}(k)Z(k) + [I-\tilde{A}^{\#}(k)A(k)]\hat{x}(k|0)\\ &= \tilde{A}^{\#}(k)A(k)x_T(k) + \tilde{A}^{\#}(k)N(k) + [I - \tilde{A}^{\#}(k)A(k)]\hat{x}(k|0)\\ &= \tilde{A}^{\#}(k)A(k)x_O(k) = [I - \tilde{A}^{\#}(k)A(k)]\hat{x}(k|0);\end{aligned} \tag{77}$$

or, alternatively, the error on the first leg is

$$\hat{x}_e(k|k) = [I - \tilde{A}^{\#}(k)A(k)][x_T(k) - \hat{x}_T(k|0)] - \tilde{A}^{\#}(k)N(k)$$

$$= x_T(k) - \tilde{A}^{\#}(k)A(k)x_O(k) - [I - \tilde{A}^{\#}(k)A(k)]\hat{x}_T(k|0). \tag{78}$$

When the level of noise is substantial, A'(k)A(k) becomes nonsingular; and

$$x_e(k|k) = -\tilde{A}^{\#}(k)N(k) = x_T(k) - x_O(k). \tag{79}$$

Thus, prior to an observer maneuver, it is not possible to identify the complete target state and the TMA estimate tends toward the minimum norm solution. Following a maneuver, equation (69) has an additional term and the estimate approaches the actual target state. The effect on the solution generated by the algorithm of table 2 is given by equation (65) and can be shown to produce a bias that fades as the number of measurements increases. Substituting equation (21) into equation (45) yields

$$\hat{x}_T(k|k) = x_T(k) + A^{\#}(k)N(k), \tag{80}$$

which reveals an additional source of bias. Since both $A^{\#}(k)$ and N(k) are functions of the measurement noise $\nu(k)$, the expectation of the second term is non-zero. This bias is structural and not inherent in nature; it is a common occurrence in parameter estimation problems in control theory,[18] and in the linear prediction techniques of signal processing.[19]

EXPERIMENTAL RESULTS

Representative target-observer geometries were simulated on the AN/UYK-7 computer in the Systems Analysis Laboratory at the Naval Underwater Systems Center. White Gaussian noise with zero mean and 0.5° standard deviation was added to the data generated by the dynamic model as shown in figure 4. Preprocessing of the target bearing was simulated by averaging twenty 1-second samples to provide a bearing measurement for a single (moving) observer target motion analysis algorithm.

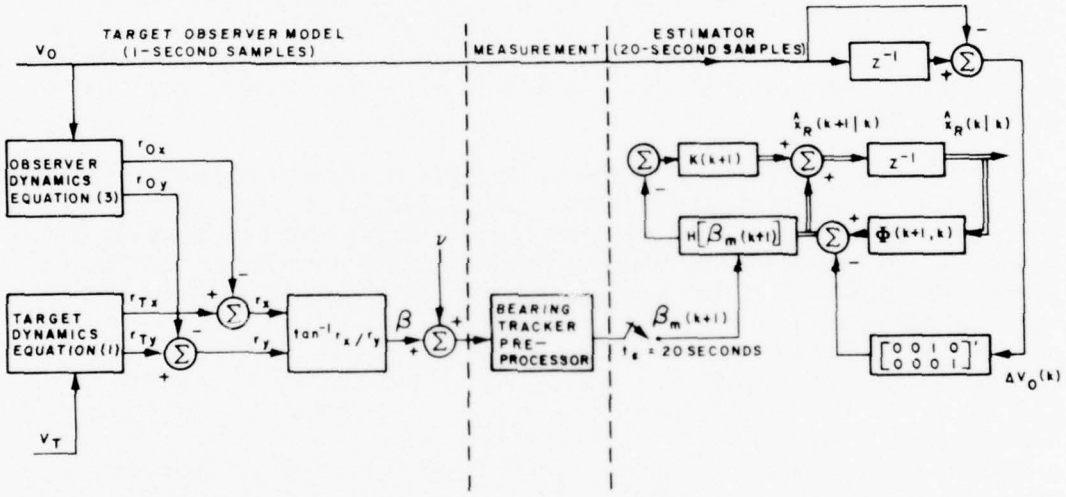

Figure 4. Simulation Diagram of Motion Analysis System

The vehicle tracks for the first target-observer geometry considered are shown in figure 5a. Both vehicles are traveling at a constant speed of 5.626 meters/second, and the observer traverses four 240-second legs involving course changes of 90°. In this first example, instantaneous or point maneuvers are used.

The relative motion plots of the solutions obtained on the first leg (shown in figure 5b) demonstrate the property of the algorithm (summarized in table 2) to provide solutions scaled by the initial range estimate under the conditions of low measurement noise and no jitter in observer velocity. Figure 5c shows the true and estimated target tracks for various initial range estimates. Note that, as predicted, the dependency of the solution on the initial range estimate fades rapidly once the process becomes observable. Figure 5d through 5g show the behavior of the components of the estimated target state $\hat{x}_R(k|k)$ as a function of elapsed time. It should be noted that, on the second leg for the particular

geometry considered, the vehicles are running parallel and the rate of change of the bearing angle is zero. Under these conditions, except for the transient immediately following the maneuver, no further improvement in the velocity estimate along the line of sight is possible and this is reflected in figures 5d and 5f.

The target motion parameters often of interest are the range, course, and speed. Plots of the range, course, and speed errors for the first example are shown in figures 6a through 6c for two initializations ($\hat{r}(0) = 10,000$ meters and $\hat{r}(0) = 0$, which is the minimum norm solution). The errors via the application of the extended Kalman filter (based on the linearization of equation (5) about a nominal trajectory, see appendix D) are also shown for purposes of comparison. Note the substantial course error and partial divergence of the range solution that occurs on the second leg when the latter method is employed. Fortunately, in this example, the situation is corrected following the next observer maneuver.

Two other encounters are shown in figures 7a through 7d and figures 8a through 8d. In both of these cases, the turning rate of the observer is constrained to 3°/second. This constraint represents the effect of finite thrust in space applications or the restricted turning rate of hydrodynamic vehicles in marine applications. In the second target-observer geometry (figure 7a), the extended Kalman filter exhibited premature collapse of the covariance matrix resulting in solution divergence. Such instability of the extended Kalman filter solution in the target motion analysis (TMA) problem was first observed by Fagin (see Murphy[2]). This instability, however, is fundamental to nonlinear modeling and is aggravated in this particular application by the fact that the estimated state used in the linearization process is not observable during the critical initial period of the problem.[17] The modeling presented in this report precludes this difficulty. Bias errors in the estimate did not appear significant for the particular geometries and noise environment examined.

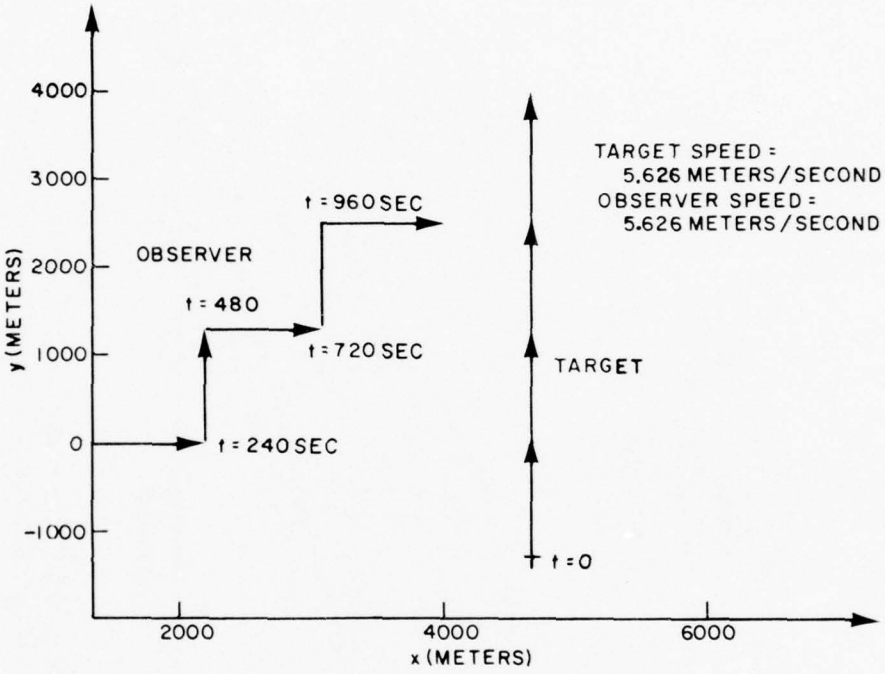

Figure 5a. Vehicle Tracks for Target-Observer Geometry No. 1

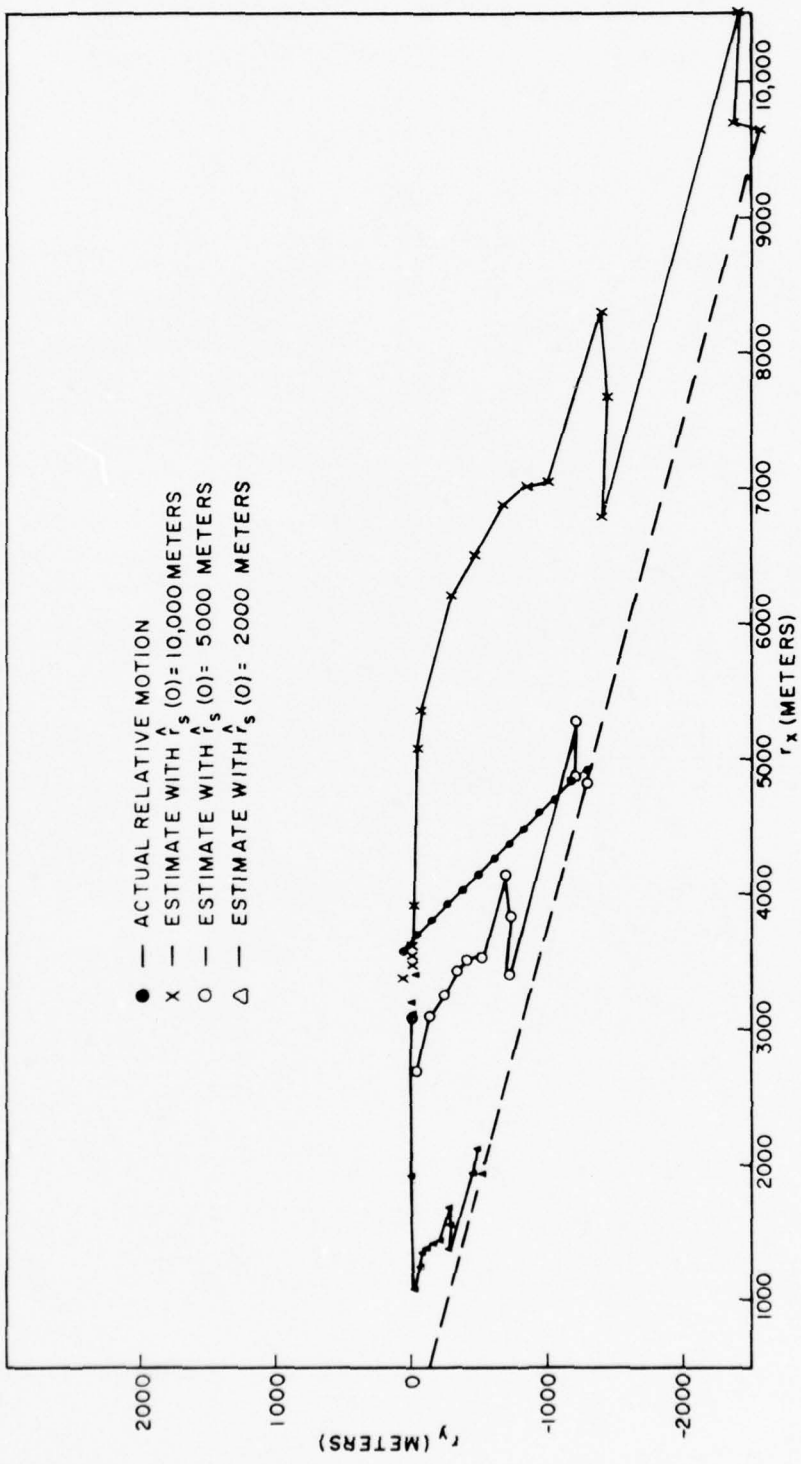

Figure 5b. Actual and Estimated Relative Motion During the First Leg for Various Initial Range Estimates (Geometry No. 1)

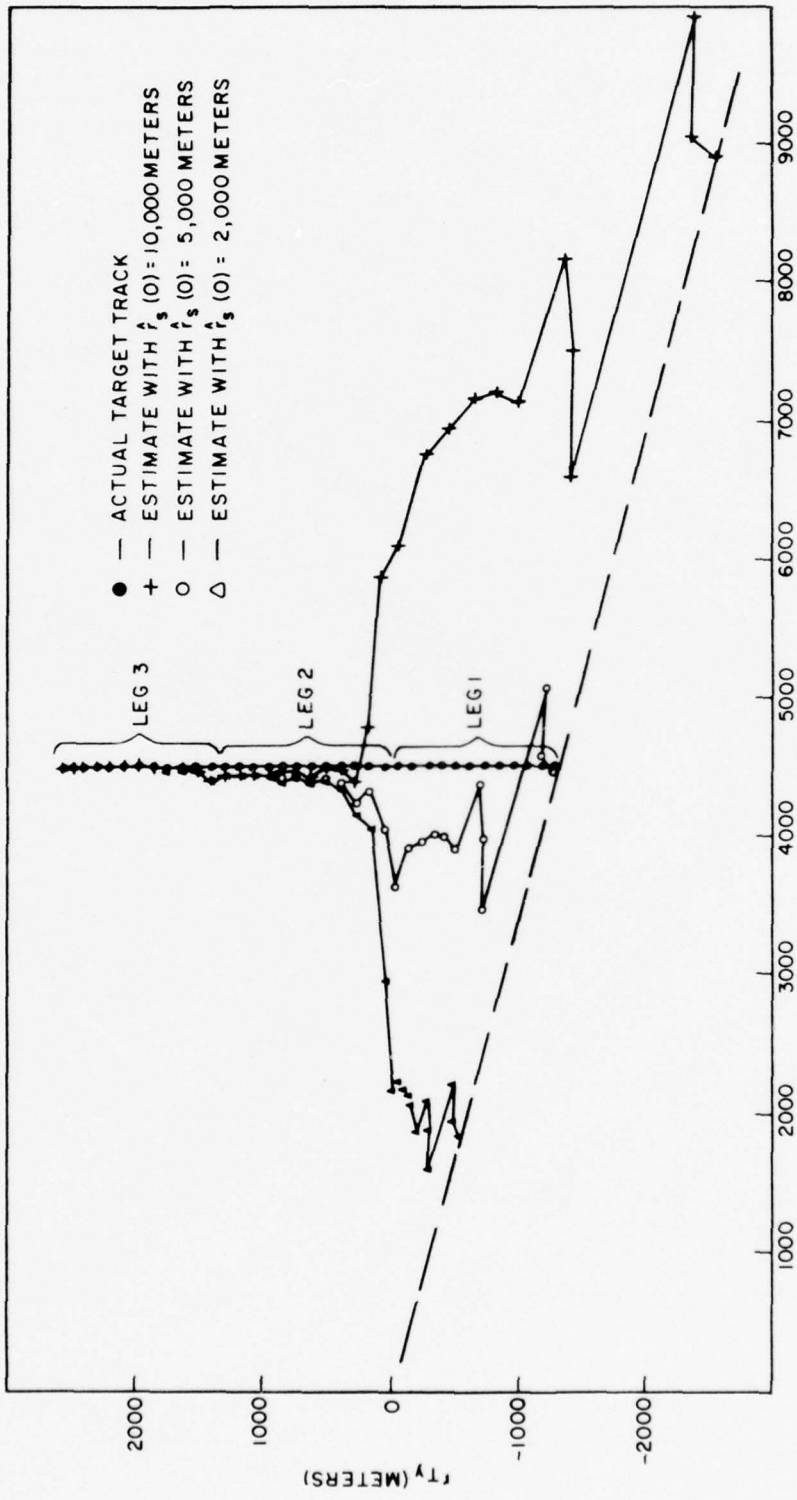

Figure 5c. Actual and Estimated Target Tracks for Various Initial Range Estimates (Geometry No. 1)

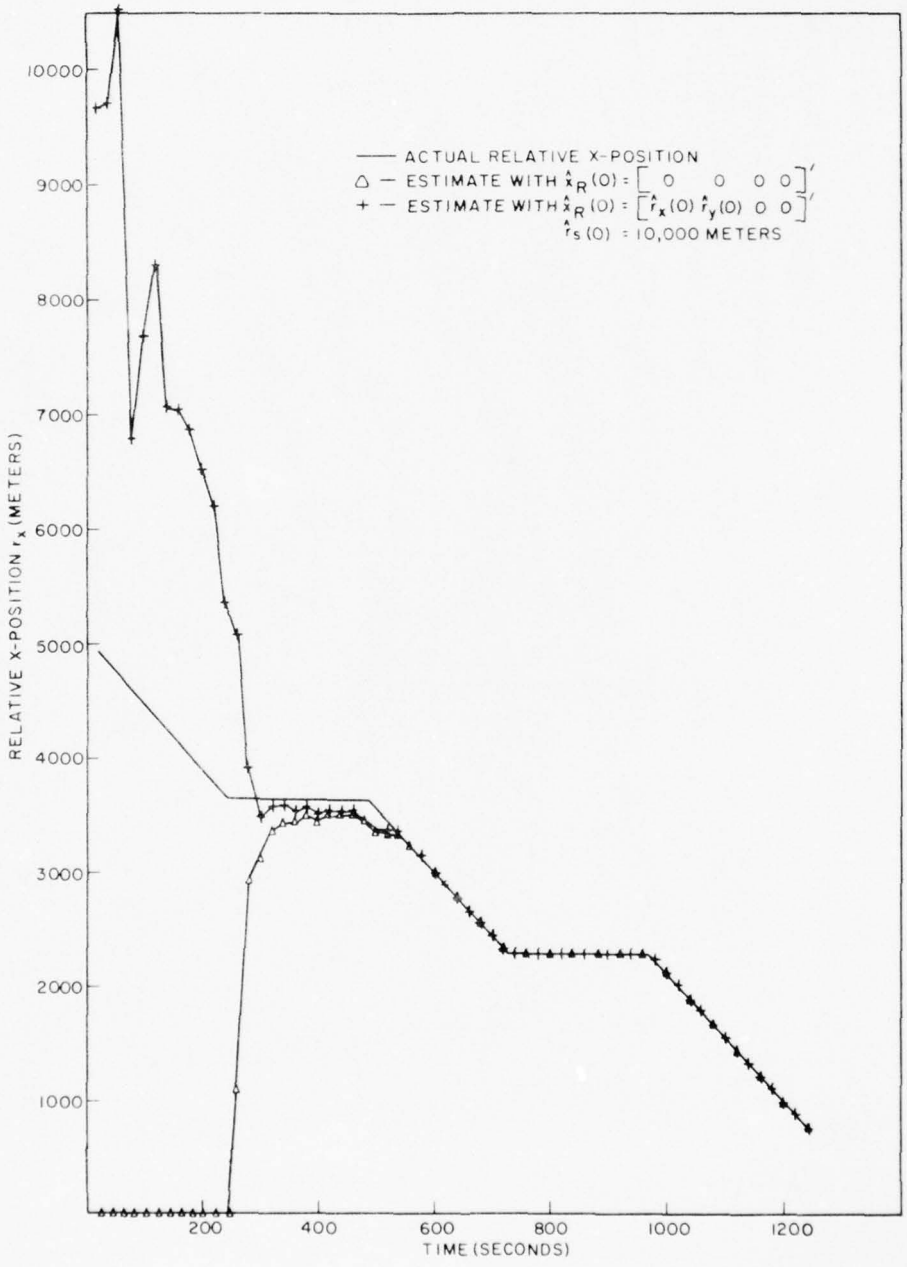

Figure 5d. Actual and Estimated Relative X-Position (r_X) as a Function of Flapsed Time (Geometry No. 1)

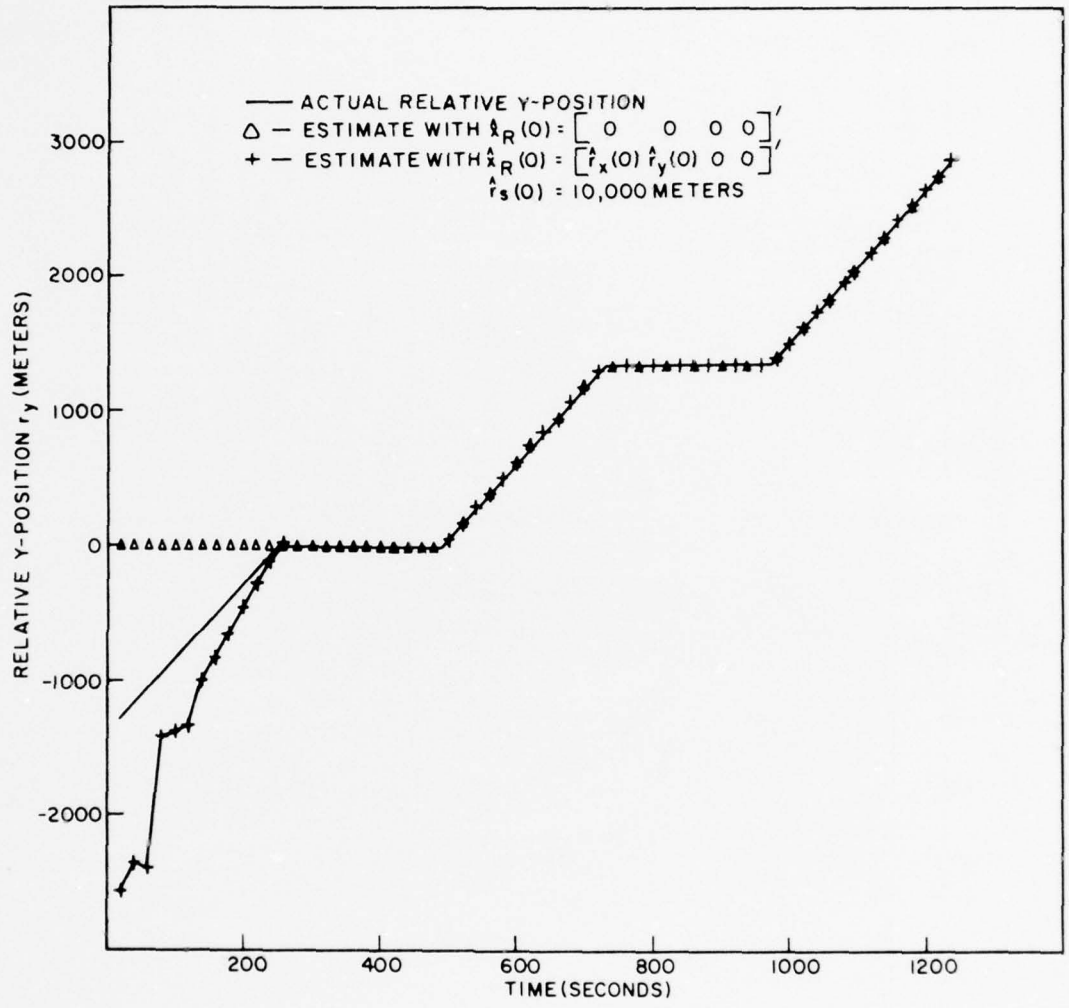

Figure 5e. Actual and Estimated Relative Y-Position (r_y) as a Function of Elapsed Time (Geometry No. 1)

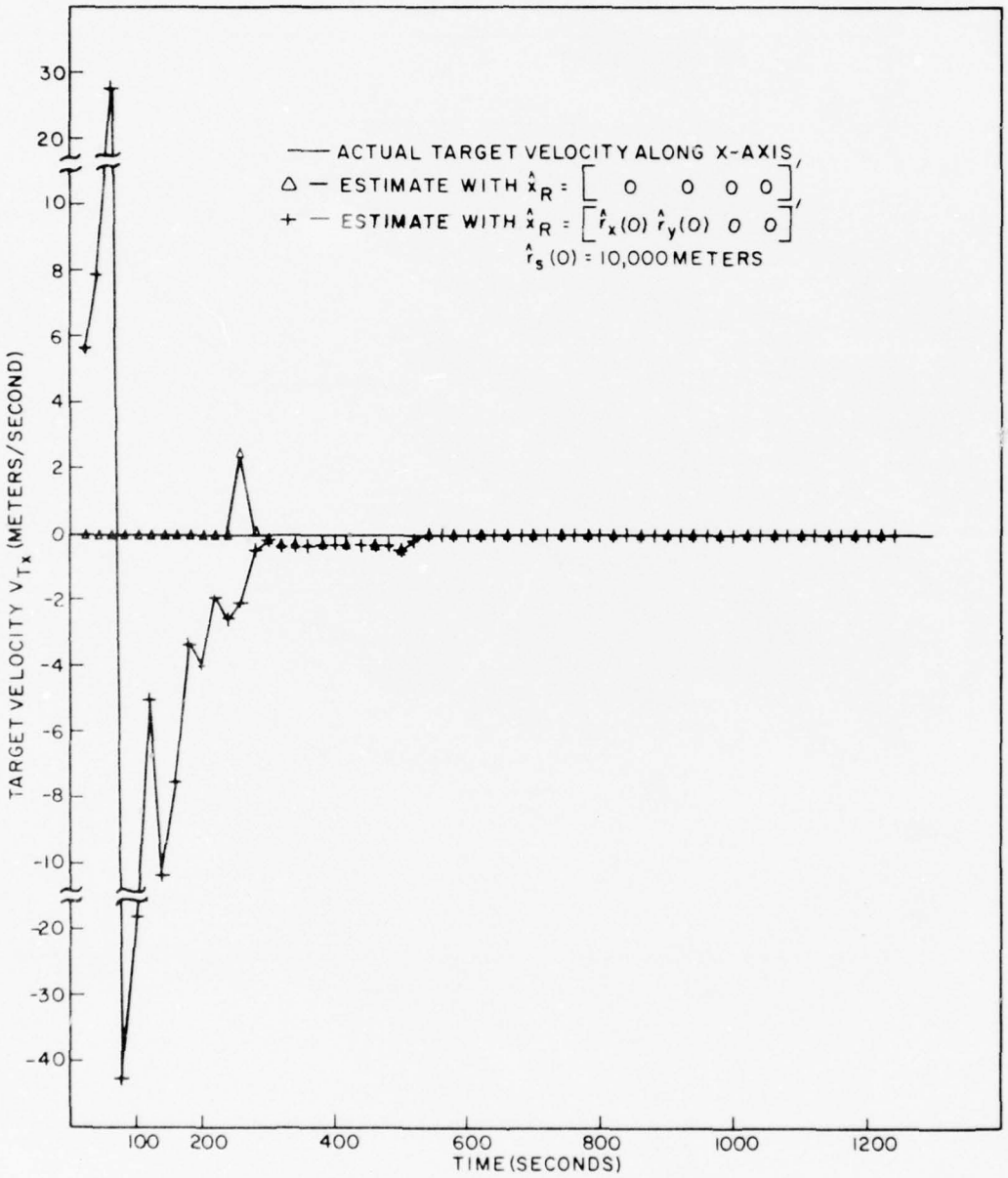

Figure 5f. Actual and Estimated Target Velocity Along the X-Axis (Geometry No. 1)

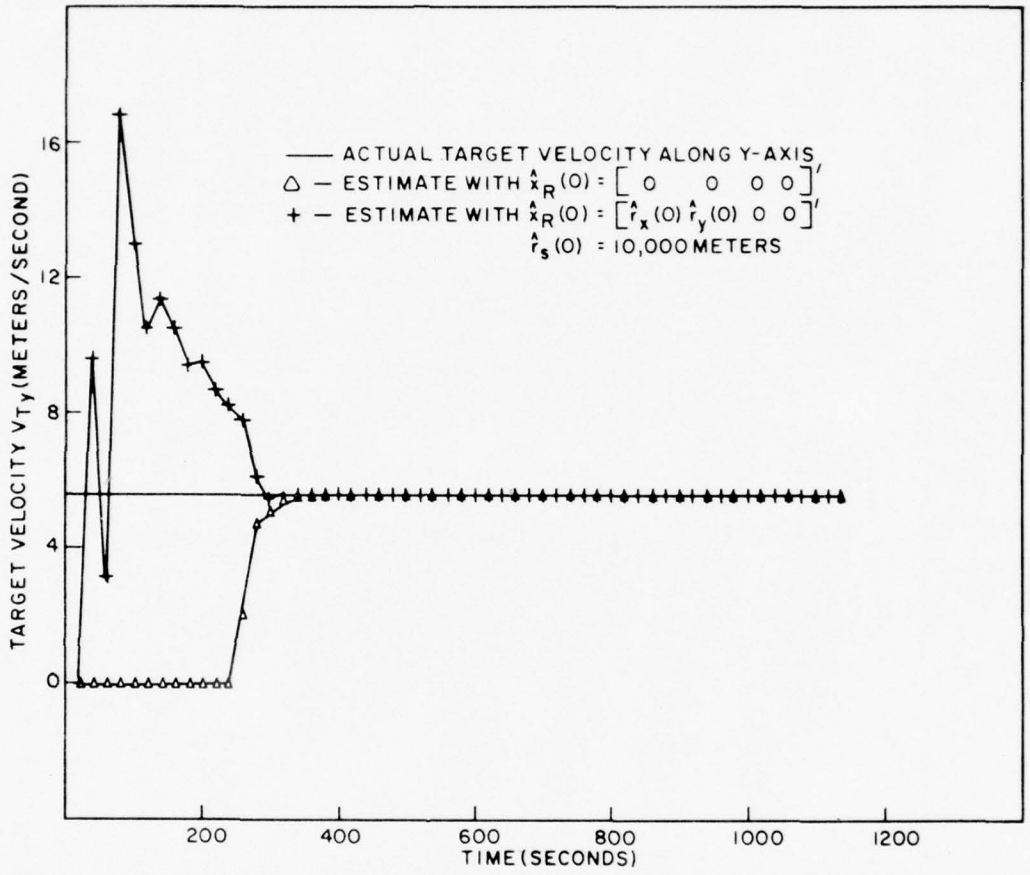

Figure 5g. Actual and Estimated Target Velocity Along the Y-Axis (Geometry No. 1)

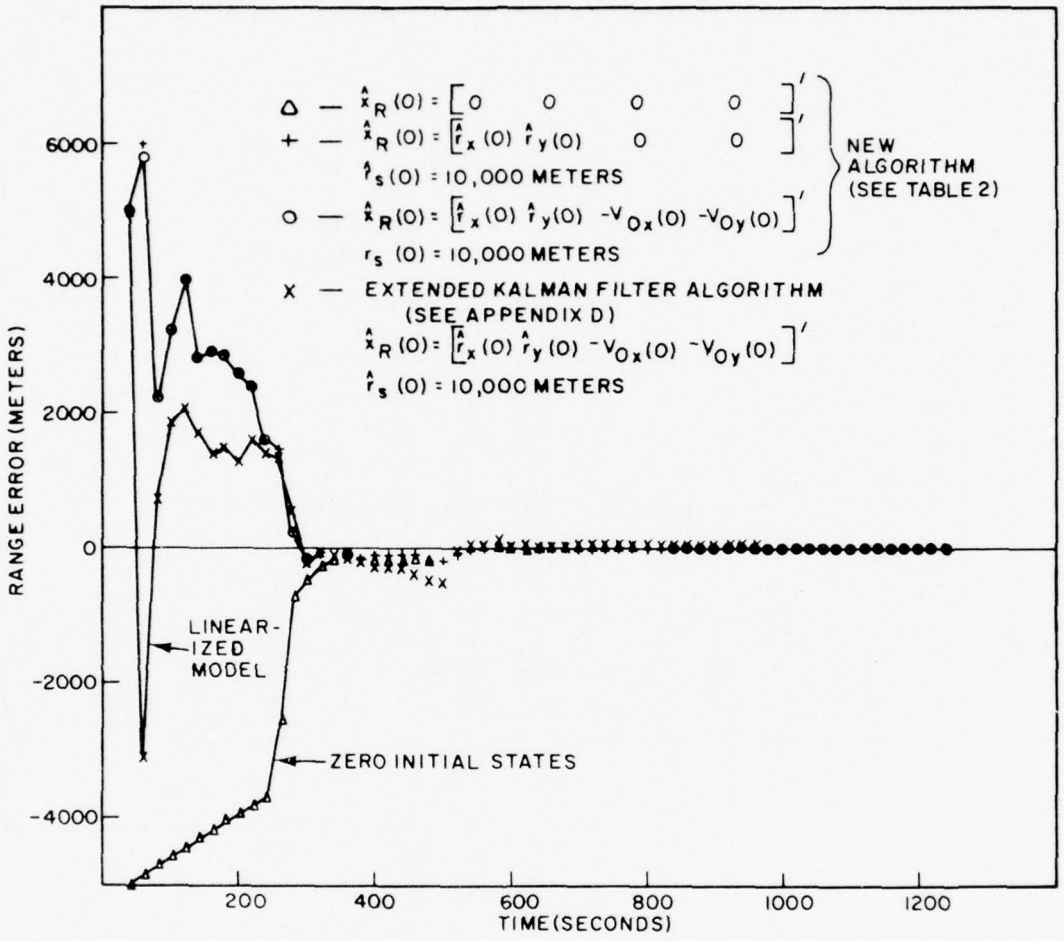

Figure 6a. Range Error for Various Initialization Parameters (Geometry No. 1)

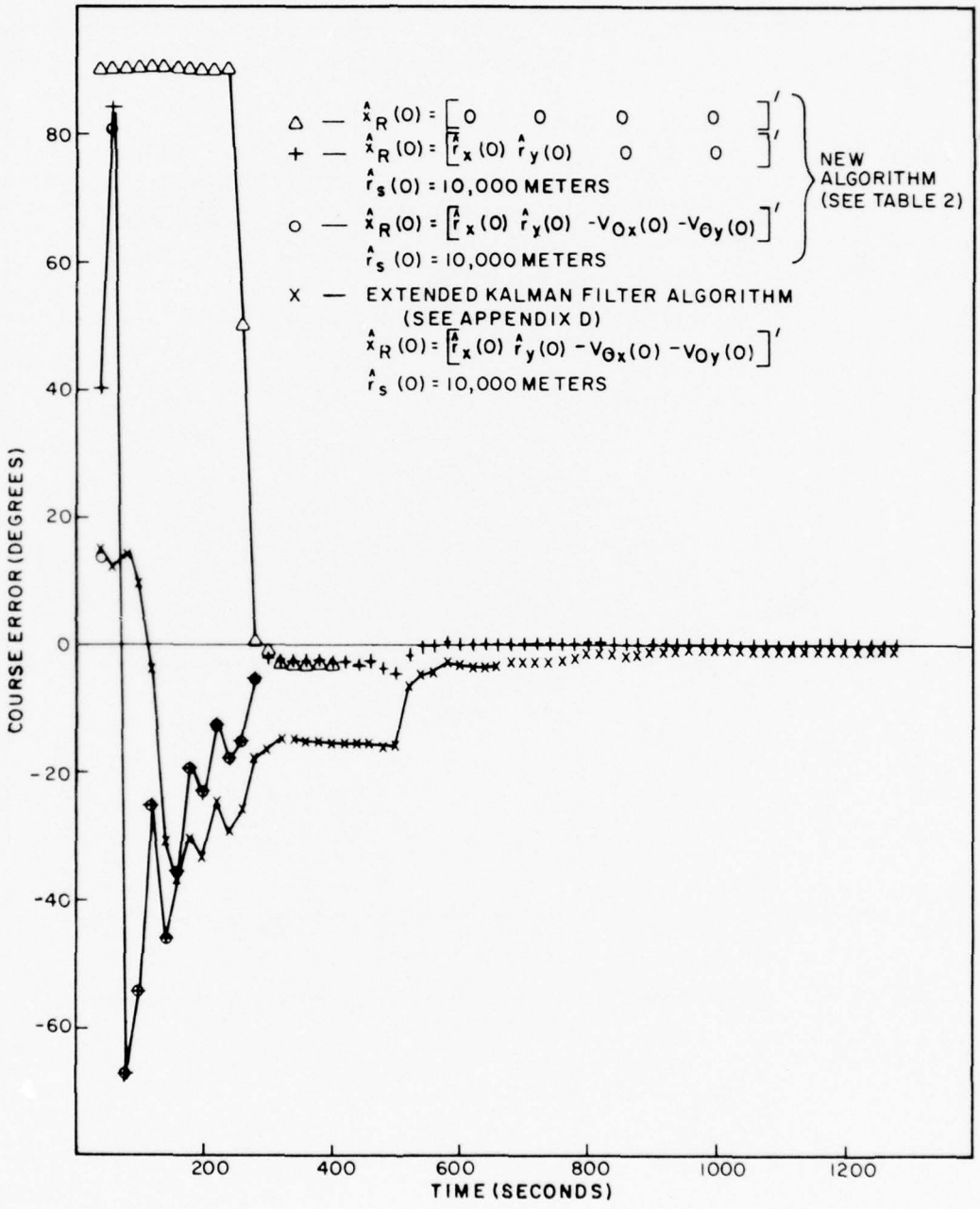

Figure 6b. Target Course Error for Various Initialization Parameters (Geometry No. 1)

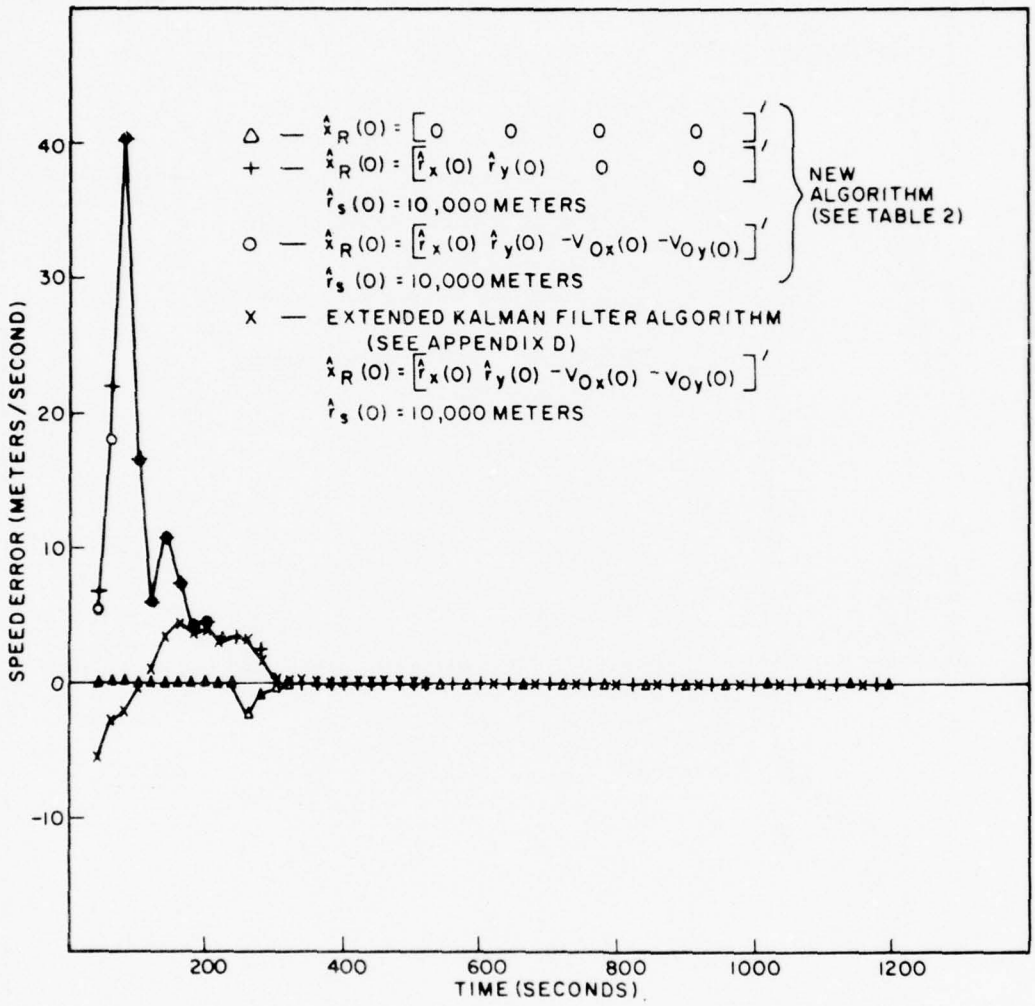

Figure 6c. Target Speed Error for Various Initialization Parameters (Geometry No. 1)

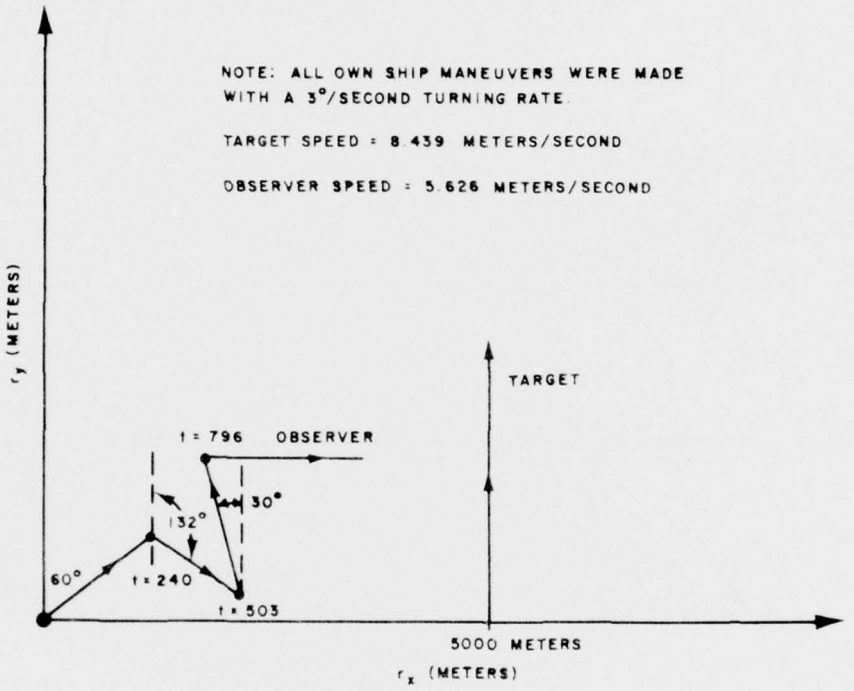

Figure 7a. Vehicle Tracks for Target-Observer Geometry No. 2

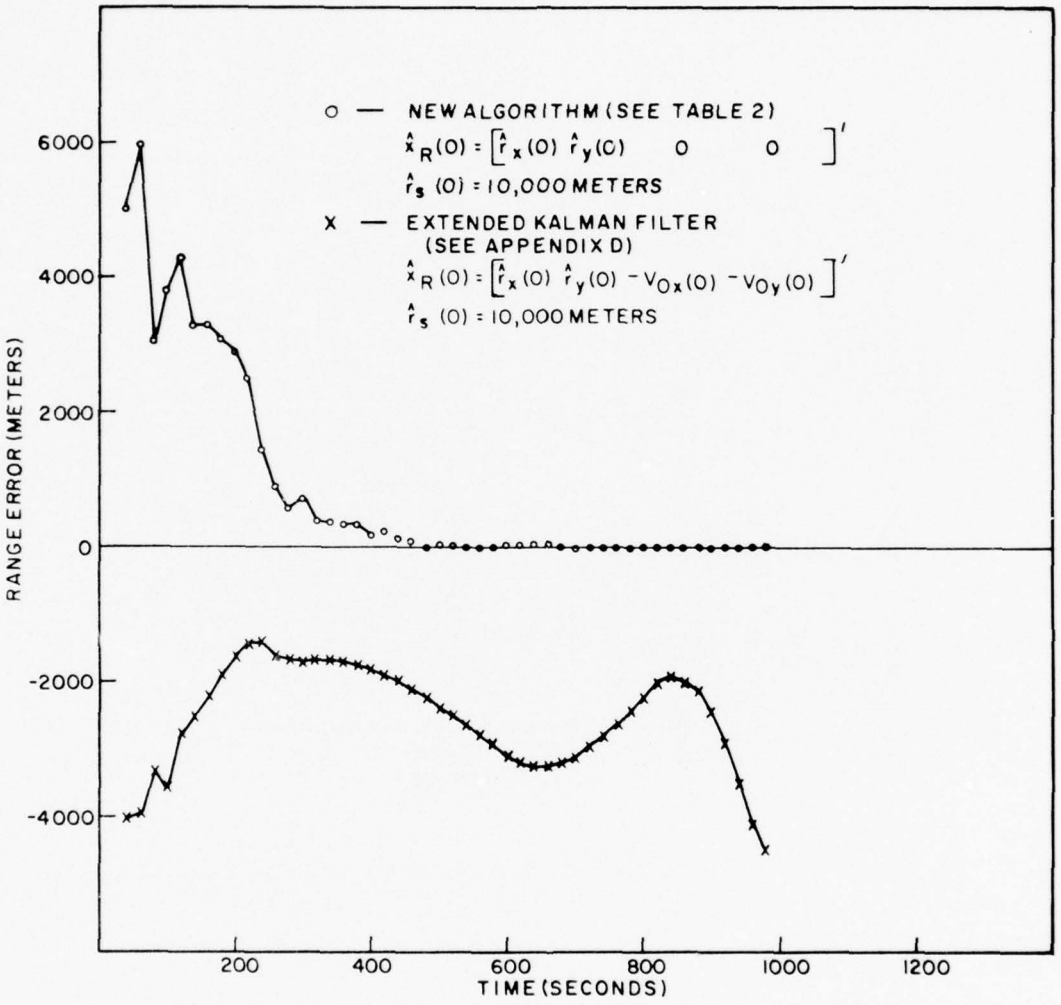

Figure 7b. Range Error for Geometry No. 2

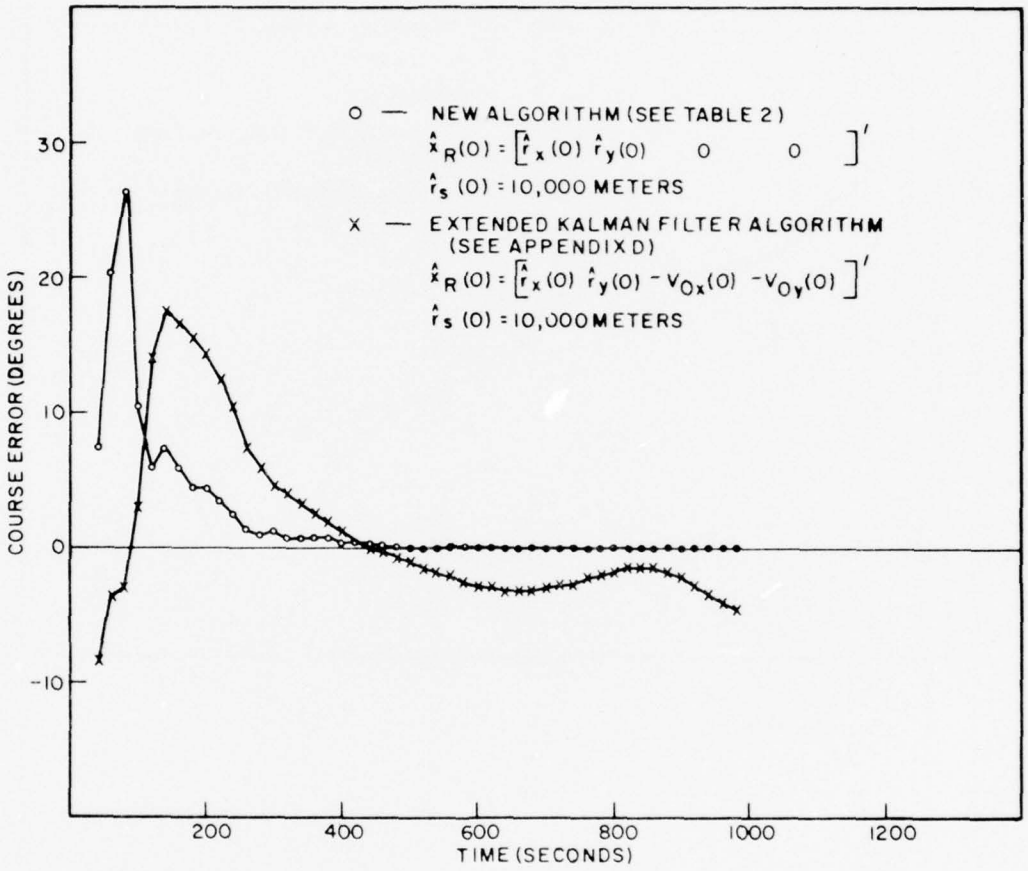

Figure 7c. Target Course Error for Geometry No. 2

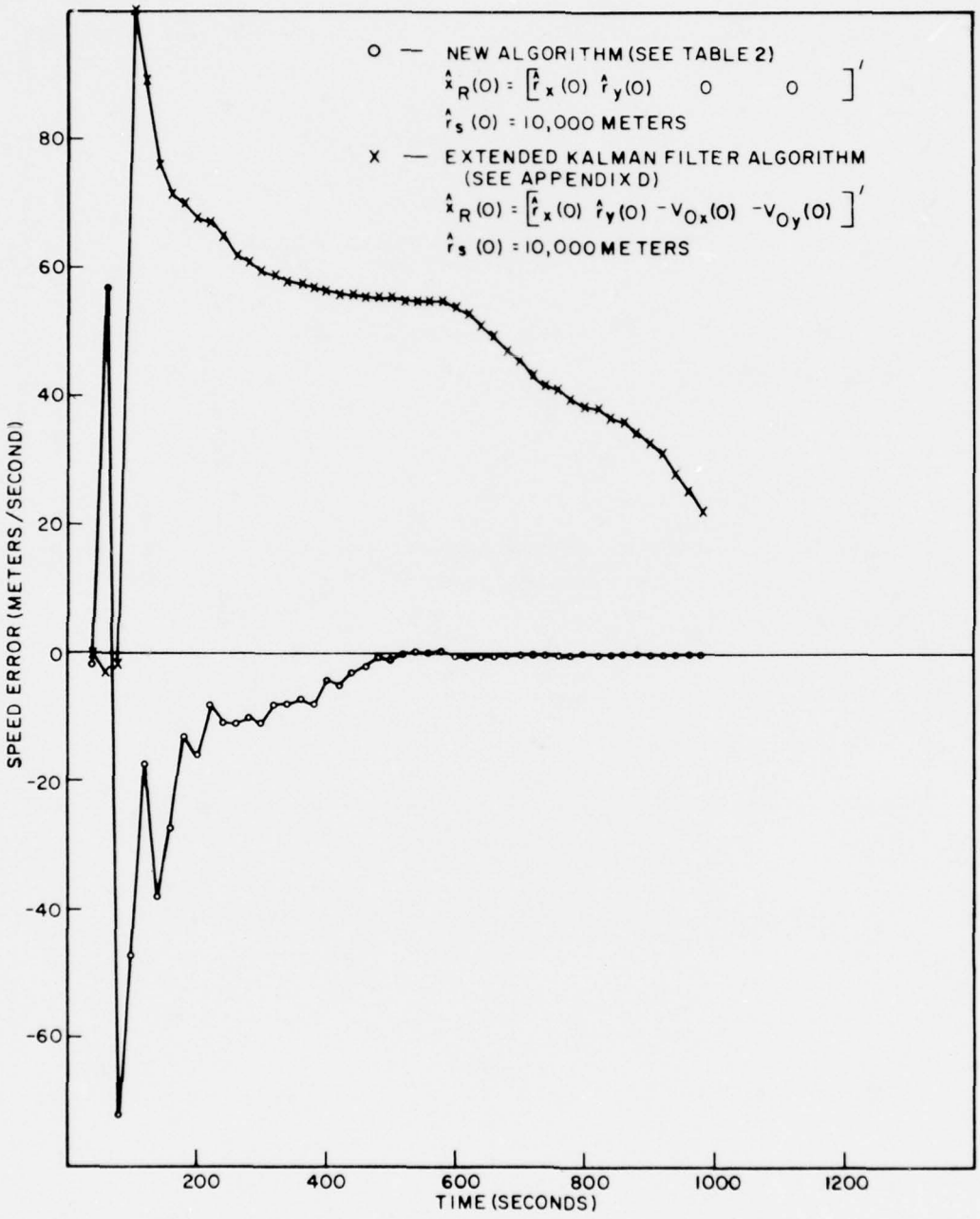

Figure 7d. Target Speed Error for Geometry No. 2

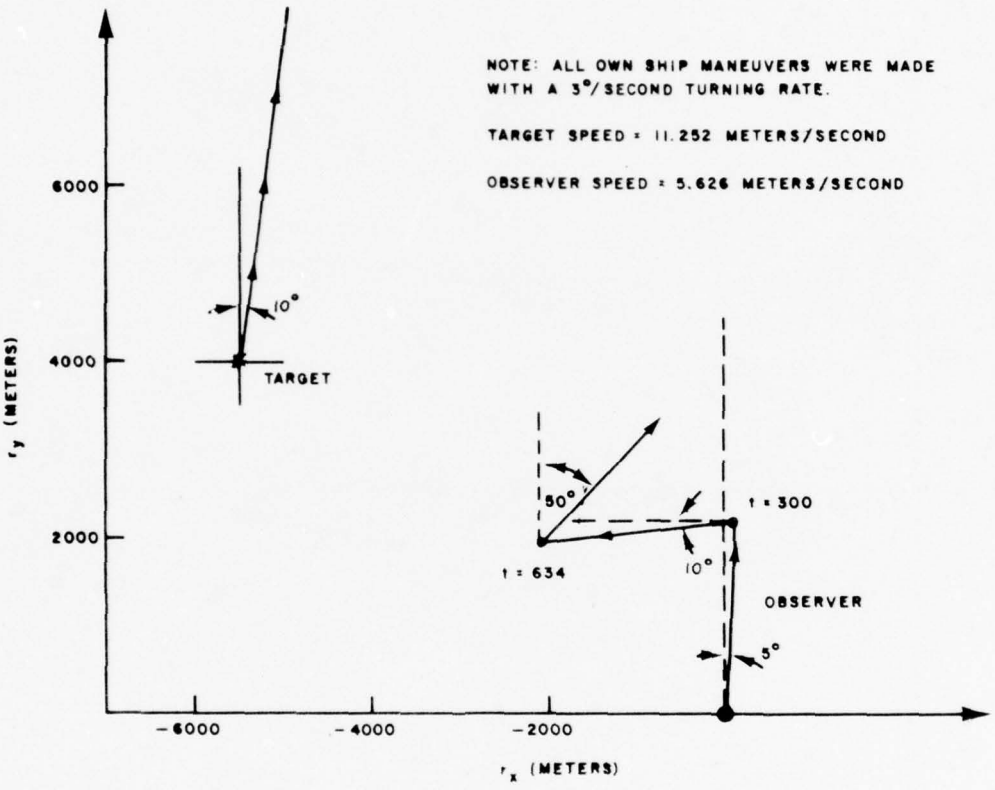

Figure 8a. Vehicle Tracks for Target-Observer Geometry No. 3

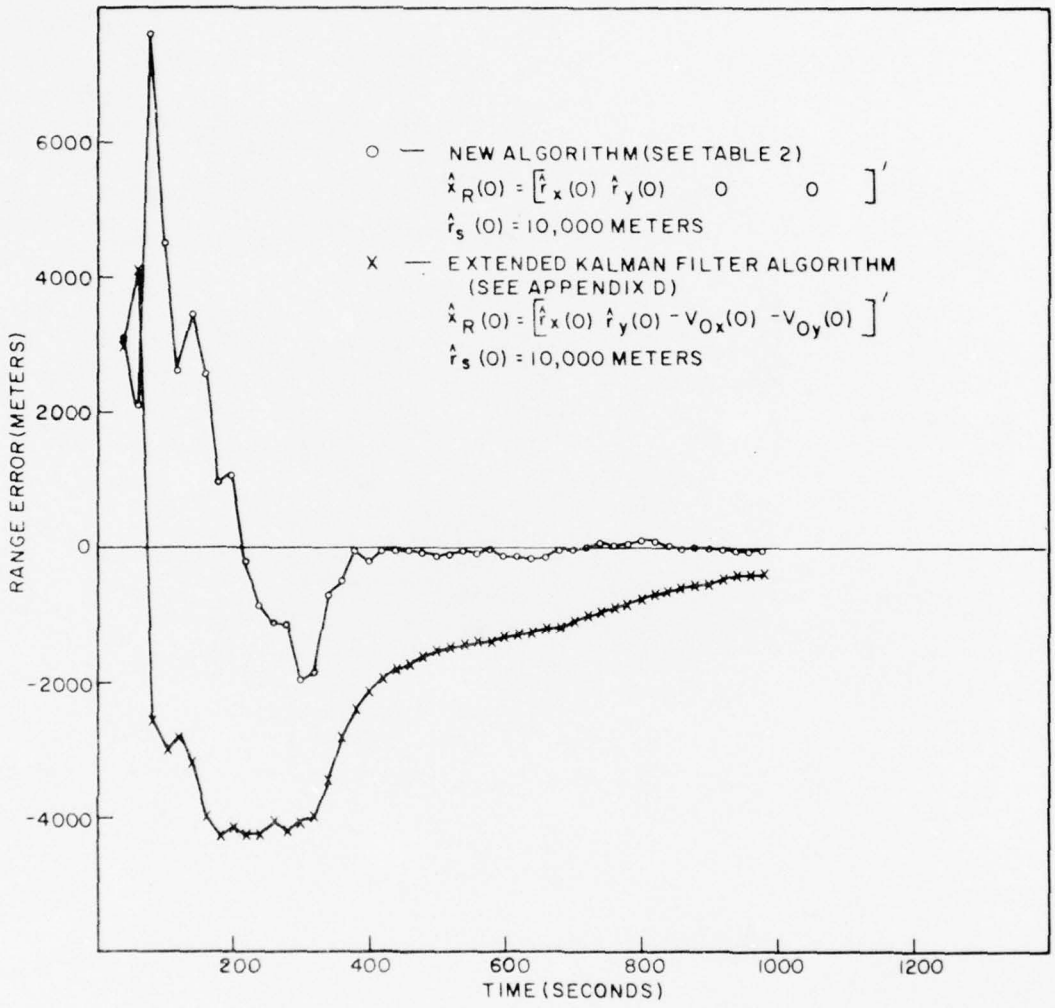

Figure 8b. Range Error for Geometry No. 3

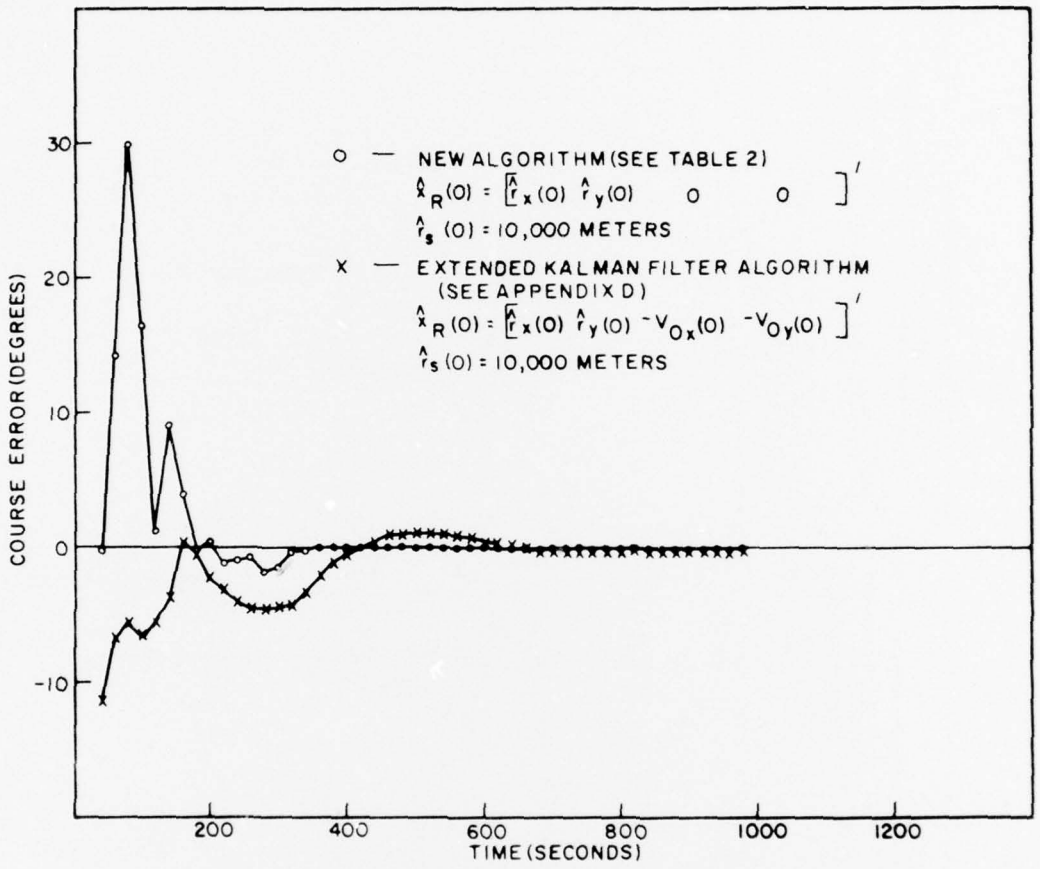

Figure 8c. Target Course Error for Geometry No. 3

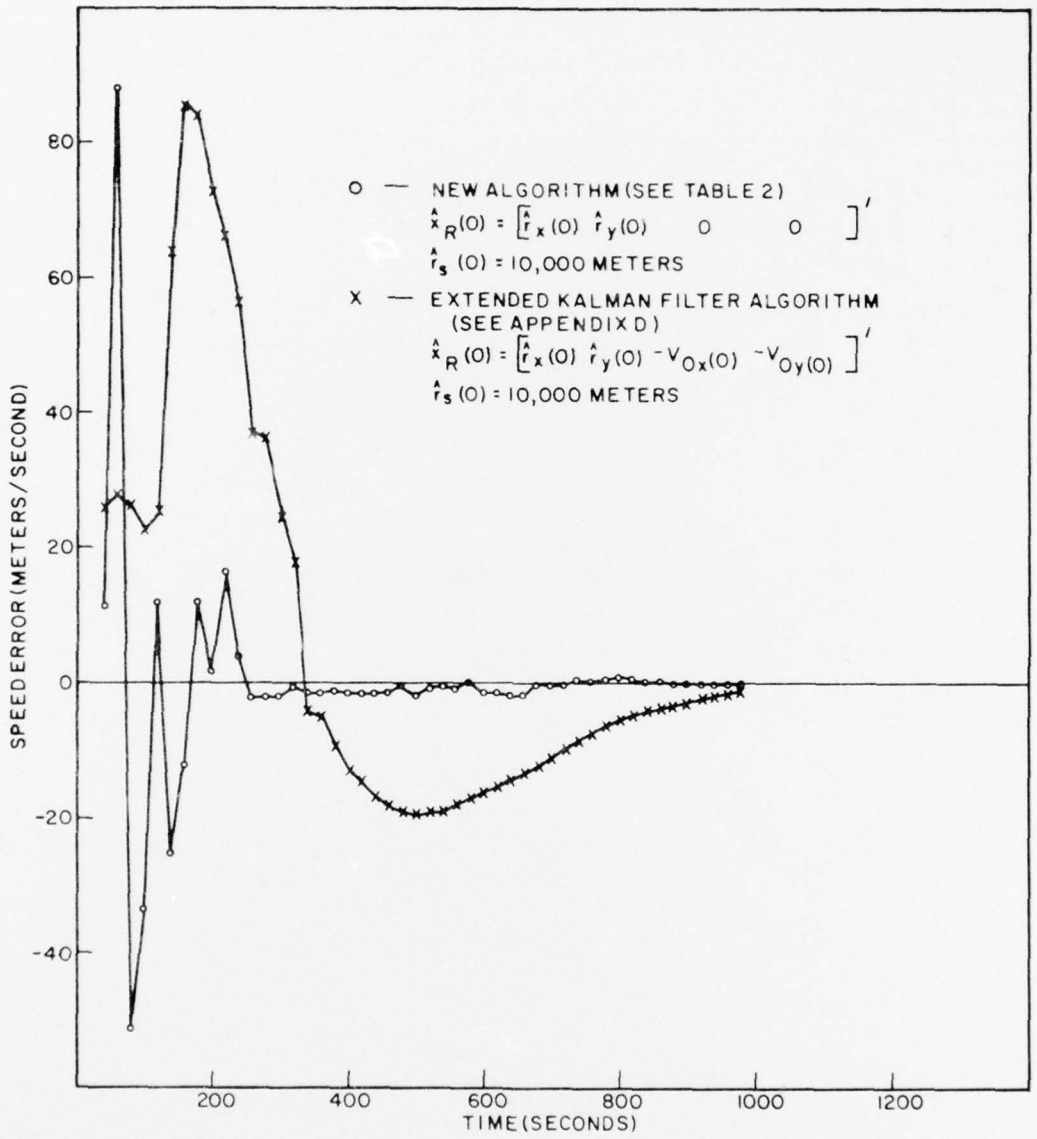

Figure 8d. Target Speed Error for Geometry No. 3

SUMMARY AND CONCLUSIONS

Bearings-only motion analysis is modeled in the form of a linear state estimation problem when the measurements are generated from the bearing observations via equation (12). Implementation of equation (12) requires knowledge of the emitter's bearing, location of the observer, and time of observation. For the special case of a single moving observer, emphasized in this report, the resulting dynamic process is unobservable on the first leg. The relationship between recursive least-squares and Kalman filtering when the dynamic process is unobservable is detailed. An estimation algorithm (table 2), including initialization, is presented that exhibits consistent behavior for all target-observer geometries examined. Minimum norm solutions are provided on the first leg of the problem; and convergence to the complete solution is achieved following maneuvers by the observer that result in the dynamic process becoming observable. Convergence of the estimate of target state is dependent upon the velocity variation undertaken by the observing vehicle. No attempt was made in this report to optimize the observer maneuvers to improve convergence. This is an area for further study.

Since the gain and covariance matrices are dependent only upon the measured bearings, changes in target velocity have the same effect on these quantities as observer maneuvers. Thus, evasive action by the target can produce false solutions and convergence of the covariance matrix. Random perturbation in the target velocity can be handled by the addition of plant noise to the model of equation (1). When the heading changes undertaken by the observer are sufficiently large, the angle tracking may require new antenna systems; and the problem is further complicated by the addition of bias errors introduced between the data legs. The more general three-dimensional problem using additional passive sensor inputs is currently under study.

REFERENCES

1. R. C. Kolb and F. H. Hollister, "Bearing-Only Target Estimation," Proceedings of the First Asilomar Conference on Circuits and Systems, 1967, pp. 935-046.

2. D. J. Murphy, Noisy Bearings-Only Target Motion Analysis, Ph.D. Dissertation, Northeastern University, 1970.

3. J. L. Poirot and G. V. McWilliams, "Application of Linear Statistical Models to Radar Location Techniques," IEEE Transactions on Aerospace and Electronic Systems, Vol. AES-10, No. 6, November 1974.

4. J. L. Poirot and M. S. Smith, "Moving Emitter Classification," IEEE Transactions on Aerospace and Electronic Systems, Vol. AES-12, No. 2, March 1976.

5. D. R. Morgan, "A Target Trajectory Noise Model for Kalman Trackers," IEEE Transactions on Aerospace and Electronic Systems, Vol. AES-12, No. 3, May 1976.

6. R. A. Singer, "Estimating Optimal Tracking Filter Performance for Manned Maneuvering Targets," IEEE Transactions on Aerospace and Electronic Systems, Vol. AES-6, No. 4, July 1970.

7. R. A. Singer and K. W. Behnke, "Real-Time Tracking Filter Evaluation and Selection for Tactical Applications," IEEE Transactions on Aerospace and Electronic Systems, Vol. AES-7, No. 1, January 1971.

8. R. E. Kalman, "A New Approach to Linear Filtering and Prediction Problems," ASME Journal of Basic Engineering, March 1960, pp. 34-35.

9. A. Papoulis, Probability, Random Variables, and Stochastic Processes, McGraw-Hill, New York, N. Y., 1965.

10. William L. Brogan, Modern Control Theory, Quantum Publishers, Inc., New York, N. Y., 1974.

11. R. Deutch, Estimation Theory, Prentice-Hall, Inc., Englewood Cliffs, N. J., 1965.

12. R. E. Kalman and R. S. Bucy, "New Results in Linear Filtering and Prediction Theory," ASME Journal of Basic Engineering, March 1961, pp. 95-108.

13. A. E. Bryson Jr., and Y. C. Ho, Applied Optimal Control Theory, Ginn and Co., Waltham, Mass., 1969.

REFERENCES (Cont'd)

14. S. L. Fagin, "Recursive Linear Regression Theory, Optimum Filter Theory, and Error Analysis of Optimal Systems," IEEE Convention Record, March 1964, pp. 216-240.

15. P. L. Odell and T. O. Lewis, Estimation in Linear Models, Prentice-Hall, Inc., Englewood Cliffs, N. J., 1971.

16. R. F. Cline, "Representations for the Generalized Inverse of Sums of Matrices," Journal of the Society for Industrial and Applied Mathematics, Numerical Analysis, Series B, Vol. 2, No. 1, 1965.

17. V. J. Aidala, Personal Communication, June 1976.

18. K. Y. Wong and E. Polak, "Identification of Linear Discrete Time Systems Using the Instrumental Variable Method," IEEE Transactions on Automatic Control, vol. AC-12, no. 6, December 1967.

19. J. Makhoul, "Linear Prediction: A Tutorial Review," IEEE Proceedings, vol. 63, no. 4, April 1975.

APPENDIX A

OBSERVABILITY OF THE NOISE-FREE TARGET-OBSERVER PROCESS

To provide insight to the behavior of the bearings-only motion analysis problem, the observability of the noise-free case is examined. Observability for time-varying systems requires that the $n \times n$ matrix

$$\sum_{i=1}^{k} [H(i)\Phi(i,k)]'[H(i)\Phi(i,k)] = A'(k)A(k) \tag{A-1}$$

be positive definite. Since the rank of the product of matrices cannot exceed the rank of individual matrices, that is,

$$\text{Rank } (AB) \leq \text{Rank } (A) \text{ or Rank } (B), \tag{A-2}$$

$$\text{Rank } (A'A) = \text{Rank } (A), \tag{A-3}$$

the system is unobservable if the rank of $A(k)$ is less than the number of states, which is four in the two-dimensional motion analysis problem. From equations (1), (11), and (22) we have

$$A(k) = \begin{bmatrix} H(k) \\ H(k-1)\Phi(k-1,k) \\ H(k-2)\Phi(k-2,k) \\ \cdot \\ \cdot \\ \cdot \\ H(1)\Phi(1,k) \end{bmatrix}$$

$$= \begin{bmatrix} \cos\beta(k) & -\sin\beta(k) & 0 & 0 \\ \cos\beta(k-1) & -\sin\beta(k-1) & -t_s\cos\beta(k-1) & t_s\sin\beta(k-1) \\ \cos\beta(k-2) & -\sin\beta(k-2) & -2t_s\cos\beta(k-2) & 2t_s\sin\beta(k-2) \\ \cdot & \cdot & \cdot & \cdot \\ \cdot & \cdot & \cdot & \cdot \\ \cdot & \cdot & \cdot & \cdot \\ \cos\beta(1) & -\sin\beta(1) & -(k-1)t_s\cos\beta(1) & (k-1)t_s\sin\beta(1) \end{bmatrix} \cdot \tag{A-4}$$

If the bearing rate is zero, implying $\beta(k+1) = \beta(k)$, then the first two columns and the last two columns of the matrix in equation (A-4) are linearly dependent and the rank of A(k) is two. Physically, this implies that it is not possible to determine the slant range of the target and the component of the relative velocity $V_R = V_T - V_O$ along the line of sight. For the case where the single moving observer is traveling at constant velocity and $d\beta/dt \neq 0$, the rank of A(k) can be shown to be three. To determine that the matrix A(k) does not achieve full rank prior to observer maneuvers, note from equations (12) and (13) that in the noise-free case

$$H(k)x_R(k) = [0], \tag{A-5}$$

where the behavior of the relative target state (constant observer velocity) is defined by

$$x_R(k+1) = \Phi(k+1, k)x_R(k). \tag{A-6}$$

By comparing equations (A-5) and (A-6) with equations (19) and (20), one obtains an equation that is similar to equation (21); that is,

$$A(k)x_R(k) = [0], \tag{A-7}$$

or

$$A'(k)A(k)x_R(k) = [0]. \tag{A-8}$$

It is clear that in order for equation (A-8) to be satisfied, either the trivial solution $x_R(k) = [0]$ is unique or A(k) is not of full rank, in which case nontrivial solutions $\hat{x}_R(k) \neq 0$ exist. However, from equation (5) one has

$$\beta(t) = \tan^{-1}\frac{V_{xt}+r_x(0)}{V_{yt}+r_y(0)}$$

$$= \tan^{-1}\left[\left(\frac{V_x}{r_s(0)}t + \sin\beta(0)\right)\Big/\left(\frac{V_y}{r_s(0)}t + \cos\beta(0)\right)\right], \tag{A-9}$$

and it is clear that a one-parameter family of solutions, scaled by $\hat{r}_s(0)$, exists. This situation is illustrated in figure A-1. Consequently, the rank of the matrix A'(k)A(k) is not equal to four, and the system is not observable during the first phase (leg) of the bearings-only motion analysis problem. For the system to become observable, an additional linearly independent measurement is required; this is realized by a change in the velocity of the observer (i.e., by an observer maneuver).

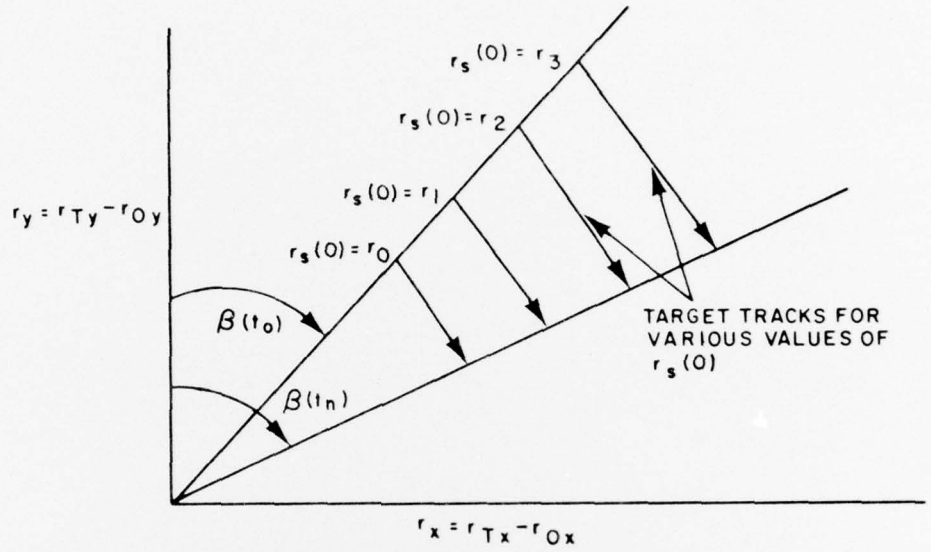

Figure A-1. Existence of a One-Parameter Family of Solutions Scaled by $\hat{r}_S(0)$ in the First Leg of the Bearings-Only Motion Analysis Problem (Stationary Observer)

APPENDIX B
MATRIX INVERSION IDENTITIES

Given the $n \times n$ positive definite matrix P, the $m \times n$ matrix A, and the $m \times m$ positive definite matrix R, then

$$PA'[R + APA']^{-1} = [P^{-1} + A'R^{-1}A]^{-1}A'R^{-1}, \tag{B-1}$$

and

$$[P^{-1} + A'R^{-1}A]^{-1} = P - PA'[R + APA']^{-1}AP. \tag{B-2}$$

Proof:

1. Pre- and post-multiply equation (B-1) by the nonsingular matrices $[P^{-1} + A'R^{-1}A]$ and $[R + APA']$, respectively.

2. Substitute equation (B-1) into (B-2), yielding,

$$[P^{-1} + A'R^{-1}A]^{-1} = P - [P^{-1} + A'R^{-1}A]^{-1}A'R^{-1}AP,$$

and pre-multiply by the nonsingular matrix $[P^{-1} + A'R^{-1}A]$.

APPENDIX C
RECURSIVE COMPUTATION OF THE MINIMUM NORM SOLUTION

Given the state transition matrix

$$\phi(k+1,k) = [I - K(k+1)H(k+1)]\Phi(k+1,k) \tag{C-1}$$

of the optimal estimator, the optimal gain matrix $K(k)$, and the history of measurements $Z(k) = [z(k)\ z(k-1)\ldots z(1)]'$, then

$$\sum_{j=1}^{k} \phi(k,j)K(j)z(j) = \widetilde{A^{\#}}(k)Z(k), \text{ and}$$

$$\phi(k,0) = [I - \widetilde{A^{\#}}(k)A(k)]\Phi(k,0). \tag{C-2}$$

Proof:

1. Rewrite equation (C-1) in the form

$$\phi(k+1,k) = [I - K(k+1)H(k+1)]P(k+1|k)P^{-1}(k+1|k)\Phi(k+1,k). \tag{C-3}$$

Utilizing the relations

$$P(k+1|k+1) = [I - K(k+1)H(k+1)]P(k+1|k), \tag{C-4}$$

$$\Phi^{-1}(k+1,k) = \Phi(k,k+1), \tag{C-5}$$

and

$$P^{-1}(k+1|k) = \Phi^{T}(k,k+1)P^{-1}(k|k)\Phi(k,k+1), \tag{C-6}$$

the optimal state transition matrix can be expressed as

$$\phi(k+1,k) = P(k+1|k+1)\Phi'(k,k+1)P^{-1}(k|k), \tag{C-7}$$

or

$$\phi(k,j) = P(k|k)\Phi'(j,k)P^{-1}(j|j), \tag{C-8}$$

for all values of j. Since

$$K(j) = P(j|j)H'(j)/\sigma_j^2, \tag{C-9}$$

the product $\phi(k, j)K(j)$ is given by

$$\phi(k, j)K(j) = P(k|k)\Phi'(j, k)P^{-1}(j|j)P(j|j)H'(j)/\sigma_j^2$$

$$= P(k|k)\Phi'(j, k)H'(j)/\sigma_j^2. \qquad \text{(C-10)}$$

Substituting equation (C-10) into the left-hand side of equation (C-2) and expanding yields

$$\sum_{j=1}^{k} \phi(k, j)K(j)z(j) = P(k|k)\frac{H'(j)z(k)}{\sigma_k^2} + \frac{\Phi'(k-1, k)H'(k-1)z(k-1)}{\sigma_{k-1}^2}$$

$$+ \frac{\Phi'(k-2, k)H'(k-2)z(k-2)}{\sigma_{k-2}^2} + \cdots + \frac{\Phi'(1, k)H'(1)z(1)}{\sigma_1^2}$$

$$= P(k|k)A'(k)Z(k). \qquad \text{(C-11)}$$

Substitution of equation (61) into equation (C-11) completes the proof.

2. Setting $j = 0$ in equation (C-8) yields

$$\phi(k, 0) = P(k|k)\Phi'(0, k)P^{-1}(0|0). \qquad \text{(C-12)}$$

Since $P^{-1}(0|0) = \Phi'(k, 0)P_x^{-1}(k|0)\Phi(k, 0)$, it follows that

$$\phi(k, 0) = P(k|k)P_x^{-1}(k|0)\Phi(k, 0)$$

$$= \left\{P(k|k)[P_x^{-1}(k|0) + A'(k)A(k)] - P(k\,k)A'(k)A(k)\right\}\Phi(k, 0). \qquad \text{(C-13)}$$

Substituting equation (55) into equation (C-13) and recognizing that $\tilde{A}^{\#} = P(k|k)A'(k)$ yields

$$\phi(k, 0) = [I - \tilde{A}^{\#}(k)A(k)]\Phi(k, 0). \qquad \text{(C-14)}$$

APPENDIX D

SUMMARY OF THE APPLICATION OF THE EXTENDED KALMAN FILTER TO THE MOTION ANALYSIS PROBLEM

A summary of the application of the extended Kalman filter to the bearings-only motion analysis problem is presented as follows:

State Vector:

$$x(k) = [r_x(k) \quad r_y(k) \quad V_x(k) \quad V_y(k)]' \tag{D-1}$$

Initialization:

$$\hat{x}(0|0) = [\hat{r}_s(0) \sin \beta_m(0) \quad \hat{r}_s(0) \cos \beta_m(0) \quad -V_{Ox}(k) \quad -V_{Oy}(k)]' \tag{D-2}$$

$$P(0|0) = \begin{bmatrix} \sigma^2_{rx} & 0 & 0 & 0 \\ 0 & \sigma^2_{ry} & 0 & 0 \\ 0 & 0 & \sigma^2_{Vx} & 0 \\ 0 & 0 & 0 & \sigma^2_{Vy} \end{bmatrix} \tag{D-3}$$

Prediction:

$$\hat{x}(k+1|k) = \Phi(k+1,k)\hat{x}(k|k) \tag{D-4}$$

$$P(k+1|k) = \Phi(k+1,k)P(k|k)\Phi'(k+1,k) \tag{D-5}$$

$$\hat{\beta}(k+1|k) = \tan^{-1}[\hat{r}_x(k+1|k)/\hat{r}_y(k+1|k)] \tag{D-6}$$

$$\hat{r}_s(k+1|k) = [\hat{r}^2_x(k+1|k) + \hat{r}^2_y(k+1|k)]^{1/2} \tag{D-7}$$

Measurement Matrix Linearization:

$$H(k+1) = \left[\frac{\partial\beta}{\partial r_x} \quad \frac{\partial\beta}{\partial r_y} \quad \frac{\partial\beta}{\partial V_{Tx}} \quad \frac{\partial\beta}{\partial V_{Ty}}\right]_{x(k+1) = \hat{x}(k+1|k)} \tag{D-8}$$

where

$$\left.\frac{\partial\beta}{\partial r_x}\right|_{x(k+1) = \hat{x}(k+1|k)} = \cos\hat{\beta}(k+1|k)/\hat{r}_s(k+1|k) \tag{D-9}$$

$$\left.\frac{\partial \beta}{\partial r_y}\right|_{x(k+1)=\hat{x}(k+1|k)} = -\sin \hat{\beta}(k+1|k)/\hat{r}_s(k+1|k) \tag{D-10}$$

$$\frac{\partial \beta}{\partial V_{Tx}} = 0 \tag{D-11}$$

$$\frac{\partial \beta}{\partial V_{Ty}} = 0 \tag{D-12}$$

Gain Computation:

$$K(k+1) = P(k+1|k)H'(k+1)[H(k+1)P(k+1|k)H'(k+1) + \sigma_\nu^2]^{-1} \tag{D-13}$$

Updating of Estimate:

$$\hat{x}(k+1|k+1) = \hat{x}(k+1|k) + K[\beta_m(k+1) - \hat{\beta}(k+1|k)] \tag{D-14}$$

$$\begin{aligned} P(k+1|k+1) &= [I - K(k+1)H(k+1)]P(k+1|k) \\ &= P(k+1|k) - P(k+1|k)H'(k+1)H(k+1)P(k+1|k) \\ &\quad \cdot [H(k+1)P(k+1|k)H'(k+1) + \sigma_\nu^2(k+1)]^{-1} \end{aligned} \tag{D-15}$$

Estimated Target Parameters:

$$\text{Target Range} = \hat{r}_s(k+1|k+1) = [\hat{r}_x^2(k+1|k+1) + \hat{r}_y^2(k+1|k+1)]^{1/2} \tag{D-16}$$

$$\text{Target Course} = \hat{C}_T(k+1|k+1) = \tan^{-1}[\hat{V}_{Tx}(k+1|k+1)/\hat{V}_{Ty}(k+1|k+1)] \tag{D-17}$$

$$\text{Target Speed} = \hat{S}_T(k+1|k+1) = [\hat{V}_{Tx}^2(k+1|k+1) + \hat{V}_{Ty}^2(k+1|k+1)]^{1/2} \tag{D-18}$$

INITIAL DISTRIBUTION LIST

Addressee	No. of Copies
ONR (Attn: J. Smith - Code 436)	1
CNM (MAT - 0323)	1
NAVSEA (SEA-034, -064, -09G3, -660D, -660D-2, -03424 (2 copies), -03414, PMS-393)	9
NADC, Warminister	1
NSWC, White Oak (Attn: J. Faulkner)	1
NOSC, San Diego (Attn: J. Fogarty)	1
PMTC, Point Mugu (Attn: C. Irwin)	1
NPS, Monterey (Attn: H. Titus)	1
Advanced Research Project Agency, Arlington	1
DDC, Alexandria	2